

FACILITY FORM 602

64-29513	(TITLE)
64	(ACQUISITION NUMBER)
01-58705	(NASA CR OR TMX OR AD NUMBER)
13	(CATEGORY)

STUDY OF INTERFACE THERMAL CONTACT CONDUCTANCE

ERWIN FRIED

SUMMARY REPORT

003
Marshall

Prepared for
RESEARCH PROJECTS LABORATORY
NATIONAL AERONAUTICS AND SPACE ADMINISTRATION
GEORGE C. MARSHALL
SPACE FLIGHT CENTER
HUNTSVILLE, ALABAMA

MAY 1, 1964

OTS PRICE

XEROX

MICROFILM

\$

\$

GENERAL  ELECTRIC

SPACECRAFT DEPARTMENT

A Department of the Missile and Space Division
Valley Forge Space Technology Center
P.O. Box 8555 • Philadelphia 1, Penna.

507-19314

TABLE OF CONTENTS

Section	Page
1 INTRODUCTION	1-1
2 PROBLEM STATEMENT	2-1
2.1 Thermal Radiation	2-2
2.2 Interstitial Conduction	2-2
2.3 Solid Conduction	2-4
3 LITERATURE REVIEW	3-1
3.1 Contacts in Air and Other Fluids	3-2
3.2 Contacts in Vacuum	3-7
4 PROPOSED MODEL	4-1
5 EXPERIMENTAL PROGRAM	5-1
5.1 Objectives	5-1
5.2 Test Apparatus	5-1
5.3 Loading of Samples	5-6
5.4 Calorimetry	5-6
5.5 Temperature Measurement	5-11
5.6 Sample Preparation	5-14
5.7 Surface Finish Measurements	5-18
6 THERMAL TEST RESULTS	6-1
6.1 Stainless Steel 304	6-1
6.2 Magnesium	6-1
6.3 Aluminum	6-4
6.4 Copper	6-4
6.5 General Results	6-6
7 GENERAL REMARKS AND CONCLUSIONS	7-1
8 REFERENCES	8-1
9 NOMENCLATURE	9-1
Appendix A THE CONTACT MECHANISM	A-1
Appendix B SURFACE DEFINITIONS AND STANDARDS	B-1

CASE FILE COPY

LIST OF ILLUSTRATIONS

Figure		Page
4-1	Deformation Test Model	4-3
5-1	Thermal Test Apparatus Schematic	5-2
5-2	Thermal Test Apparatus	5-3
5-3	Thermal Conductance Apparatus with Sample	5-4
5-4	Thermal Conductance Apparatus with Sample and Radiation Shield.	5-5
5-5	Heater, Guard Heaters, Heatsink, and Load Button	5-8
5-6	Radiation Guard Heaters	5-9
5-7	Test Sample with Thermocouples	5-12
5-8	Thermocouple Installation Layout	5-13
5-9	Representative Temperature Gradient Curve	5-15
5-10	Vacuum System and Test Area	5-16
5-11	Typical Talysurf Trace for Sample 13	5-21
5-12	Talysurf Trace Showing Waviness (Sample 25)	5-21
6-1	Thermal Conductance vs. Contact Pressure - 304SS	6-2
6-2	Thermal Conductance vs. Contact Pressure - AZ31B Magnesium	6-3
6-3	Thermal Conductance vs. Contact Pressure - 6061-T6 Aluminum	6-5
6-4	Thermal Conductance vs. Contact Pressure - OFHC Copper	6-7
7-1	Thermal Conductance, Log-Log Plot, Stainless-Steel 304	7-1

ACKNOWLEDGEMENT

The diligent support provided by Messrs. M. Kelley, L.W. Henry of the Thermal Laboratory in the execution of the experimental program, as well as that of other General Electric Company personnel is gratefully acknowledged.

1. INTRODUCTION

The thermal-joint conductance between metallic surfaces in a vacuum has recently become of considerable interest in a number of fields where the transfer of heat between mating surfaces has to be accomplished in the absence of a conducting fluid. The most prominent of these applications include space vehicles with their environmental control subsystems, space-vehicle-energy conversion devices, as well as space environmental-simulation chambers.

Other applications include research studies, where the absence of an interstitial, conducting fluid permits observation of the solid conduction mode without extraneous effects.

It was only during the past few years that a moderate effort has been started in this area as evidenced by technical papers appearing in the literature and by academic theses being published.

This report presents the results of a predominantly experimental and concurrent analytical study of the interface thermal-contact conductance between metals in a vacuum.

The presentation starts with a discussion of the general problem, drawing on existing work in vacuum and in the presence of gases. The results of a literature survey will be presented and the various prediction methods discussed. This will be followed by a proposed approach to thermal conductance prediction, with the concurrent experimental program and experimental results presented in detail. A number of conclusions and recommendations for further work, based on this program conclude the narrative portion of this report.

2. PROBLEM STATEMENT

When two metallic surfaces are held in contact, the heat transfer between them is a function of the actual contact area, the interstitial fluid and the thermal properties of the contact surfaces. The actual contact area for nominally flat surfaces is a function of the contact pressure, the surface finish, the elastic and plastic properties of the material and, at low and moderate contact pressure, the true material flatness.

The material flatness is important, because conduction heat transfer can only take place at points of actual contact, regardless of the surface finish. Thus actual contact between surface asperities must occur, where the regions of actual contact are a function of the degree of mating between the two surfaces of interest. For this reason, surface finish may not be significant, if there exists large scale waviness or non-flatness and one could consider the waviness or macroscopic effects to be overriding in significance.

The problem of flatness deviation and waviness has been considered by a number of previous investigators (Ref. 2, 3, 4, 5, and 14), but has not been studied to the same extent as is presented by Clausing and Chao (Ref. 3). Fenech and Rohsenow (Ref. 5) also have discussed the problem but have not included it in their model of the contact.

The designations used by Clausing (Ref. 3), refer to the contacts due to surface finish as "the microscopic" and the contacts due to large scale waviness or non-flatness as the "macroscopic" contact areas. These terms will also be used in this report.

For the case of the thermal-contact conductance in a vacuum, the predominant mode of heat transfer is through the asperities making up the actual contact points, since at gas pressures of 1.3×10^{-2} Newton/m² (10^{-4} mm Hg) the free molecule conductivity in the gap represents less than 1 percent of the thermal conductivity at normal temperature and pressure.

The thermal contact conductance is defined as

$$h_c = \frac{Q/A}{\Delta T} \quad (1)$$

where Q is the heat flow rate through the contact; A is the apparent area of the contact (i. e. , the projected area of the contact perpendicular to the direction of heat flow); and ΔT is the additional temperature drop due to the interface.

The modes of heat transfer to be considered are: 1) thermal radiation, 2) gaseous, molecular or other conduction through the interstitial fluid, and 3) solid conduction through the asperities. These three heat transfer modes are interdependent and should be treated as such. However, to simplify the analysis, each mode will be treated separately. It will be seen later, that this interdependence need not be considered in this program, since radiation and interstitial conduction are negligible.

2.1 THERMAL RADIATION

The thermal radiation between the surfaces of a contact can be treated in a manner similar to parallel flat plates as is described in most heat transfer texts.

$$q = \epsilon_{1-2} \sigma (T_1^4 - T_2^4) \quad (2)$$

where:

$$\epsilon_{1-2} = \frac{1}{\frac{1}{\epsilon_1} + \frac{1}{\epsilon_2} - 1} \quad (2a)$$

This represents somewhat of a simplification, since it is based on parallel flat plates, whereas a contact really represents a number of partially closed cells. A detailed study of this problem is beyond the scope of the present program.

The thermal radiation mode is important only at very low contact pressures or at temperatures considerably above room temperature. Since all tests in this program were done near room temperature, the radiation contribution was negligible in all tests performed in this program. No numerical examples will be given here, since they are available in a number of the cited references.

2.2 INTERSTITIAL CONDUCTION

Although this study is concerned primarily with the contact conductance in a vacuum, the interstitial conduction due to fluids will be discussed as well, since it must be

considered in the case of outgassing materials or in pressurized spacecraft. Heat flow through a fluid is essentially linear, resulting in an expression of the form

$$q_f = \frac{k_f}{\delta_1 + \delta_2} (T_1 - T_2) , \quad (3)$$



where δ_1 and δ_2 represent the effective gap thickness as shown in the above sketch and T_1 and T_2 are the temperatures in a plane at distance δ_1 , δ_2 from the fictitious centerline or datum plane.

It is evident that considerable difficulty will be encountered in evaluating δ_1 , δ_2 , although a three-dimensional graphical method may lead to a general type of solution. The problem can be compounded further, if not one but two fluids are considered such as a liquid-gas mixture in the gap. Then equation (3) must be modified to consider this effect. There presently exists no satisfactory method to determine this gap dimension for fluid conduction purposes.

For the case of a space environment, a vacuum, or rarefied gases, when the mean free path of a molecule is much greater than the distance separating the boundaries across which heat is to be transferred, intermolecular collisions are less frequent as compared to collisions with these boundaries. For example, the mean free path of air molecules is about 5 centimeter at room temperature for a pressure of 0.13 Newton/m² (10⁻³ mm Hg).

As presented in standard references, the following expression can be written for heat transfer in a rarefied gas between parallel plates:

$$q_f = a \delta \left[\frac{\gamma + 1}{\gamma - 1} \right] \left[\frac{R_o}{8\pi} \right]^{1/2} \frac{p}{(MT)^{1/2}} , \quad (4)$$

where

$$a = \frac{a_1 a_2}{a_1 + a_2 - a_1 a_2}, \quad (5)$$

which can be rewritten as an effective accommodation coefficient

$$a = \frac{1}{\frac{1}{a_1} + \frac{1}{a_2}} - 1, \quad (6)$$

which is of similar form as that for the effective emissivity between parallel plates shown in equation 2a. The mean pressure and temperature values occurring in the gap must be inserted in equation 4. The terms in equation 4 are: a , effective accommodation coefficient, $\delta = \delta_1 + \delta_2$ as used in equation 3, γ is the ratio of specific heats, and R_0 is the gas constant.

2.3 SOLID CONDUCTION

For the case of thermal contacts in vacuum, the solid conduction contribution represents the most significant part of the heat transfer mechanism for all but very low contact pressures. For this reason the greatest amount of attention will be paid to this part of the work. The solid conduction contribution can be expressed in its simplest form as:

$$q_s = \frac{k_s m}{\delta_1 + \delta_2} (T_1 - T_2), \quad (7)$$

where m is the ratio of actual to nominal contact area and includes the constriction effects, k_s is the mean solid conductivity, and T_1 , T_2 are the temperature of the mating surfaces at distances δ_1 , and δ_2 from the datum plane (the fictitious reference mid-plane).

The value of m , and in particular the actual contact area, depends on the regions within the nominal contact area which are in physical contact with each other. Thus any degree of non-flatness can affect this degree of mating between surfaces, which will increase with increasing contact pressure as a result of elastic deformation. This behavior is due to the macroscopic constriction resistance and is discussed

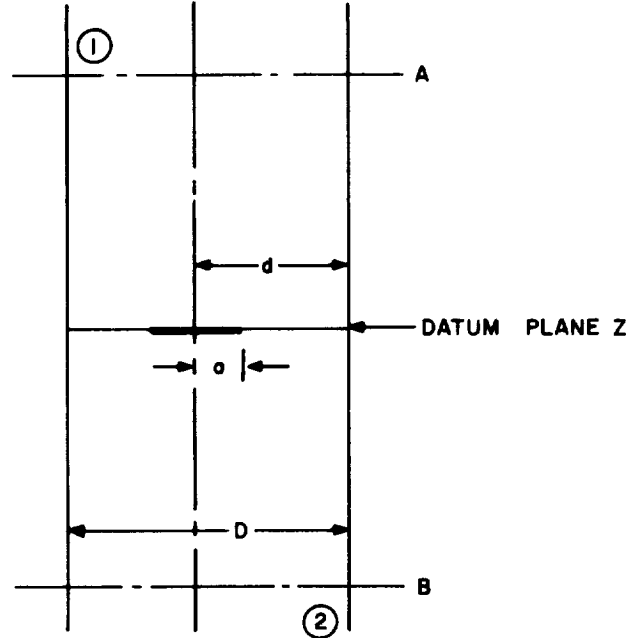
in detail in References 3 and 26. It should be noted, however, that it is not necessary for the large-scale non-flatness to be a spherical arc as is implied by the Hertz elastic model and shown in Reference 3. It can consist of several regions acting in parallel, the sum of which act similar to an elastic spherical contact. The existence of several spherical contact segments will, however, not result in an area or conductance curve identical to that of a single such segment, but should result in a curve similar to it, but displaced. Appendix A discusses some of the recent work in this area.

Unfortunately the direct determination of m , δ_1 , and δ_2 is extremely difficult by analytical or experimental means. In fact, the study of approaches to the determination of these quantities has been the subject of two doctoral dissertations recently. These are presented in References 5 and 3. One of the best and earliest fundamental studies on metal-to-metal contacts was carried out by R. Holm (Ref. 1) in a study of electric contacts. Some of the approaches shown in Reference 1 shall be utilized in order to obtain some understanding of the theory of contacts, even though it was written concerning electric contacts. Electric contacts, when perfectly clean, i.e., when no resistance due to oxide films is added, can be considered analogous to thermal contacts. In fact, such electric constriction resistance measurements can be used to obtain thermal constriction resistance data if due attention is paid to the effect of differential thermal expansion and surface effects on the actual contact area. It is the lack of adequate means to determine the latter, as well as the problem of oxide film and surface effects which creates the need for the reported work.

For example, some reported directional heat flow effects for dissimilar thermal joints (Ref. 30) has been attributed to differential thermal expansion between the asperities of the respective metal surfaces (Ref. 32). Although the phenomena occurring in dissimilar metal joints have not yet been sufficiently studied and understood, the electrical-thermal analogy could well fall down due to such purely thermal effects as differential thermal expansion of asperities.

If a cylindrical contact is considered, as shown below, where heat flows from A to B through a contact spot having radius a , some distinction must be made between the

resistance due to the thermal resistance of the material of 1 and 2 between A and B respectively and the datum plane Z, and the resistance R_c due to the contact or constriction at the datum plane itself*.



This can now be written

$$R_{\text{tot}} = R_{AB} + R_c. \quad (8)$$

Experimentally these values can be obtained by measuring the temperature difference between A and B and determining the temperature drop across the interface by extrapolation from A and B to the datum plane. Thus,

$$\Delta T_{AB} = qR_{AZ} + aR_{ZB} + qR_c \quad (9)$$

where:

$$R = \frac{x}{k}, \quad (10a)$$

*Although there is some controversy on the applicability of the terms contact resistance, constriction resistance and the complementary term contact or constriction conductance, these terms will be used in this report interchangeably, since there really is no conflict in their meaning within the context of this work.

or,

$$R_c = \frac{1}{h_c} , \quad (10b)$$

and x is the dimension of the solid conduction path of interest.

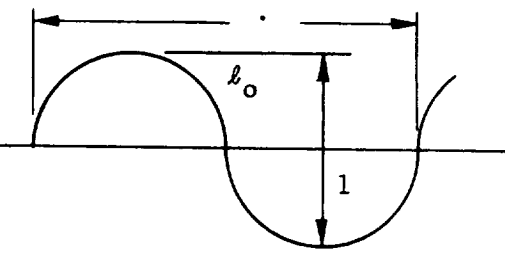
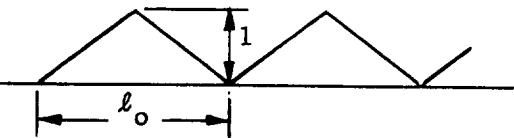
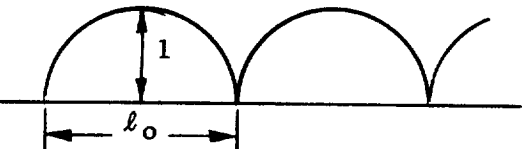
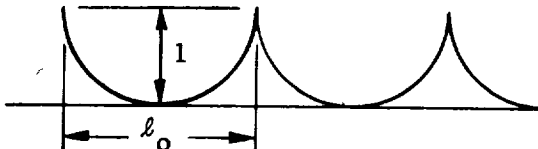
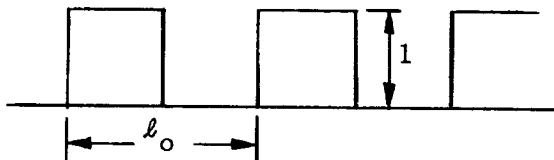
Since the thermal conductivity of many materials is temperature dependent, the value of k used in this calculation should be based on the local average temperature of the specimen.

The value of the term m , the ratio of actual to nominal contact area as shown in equation (7) still needs to be determined. The approaches proposed in this study for this determination are shown in Section 4.

In both cases Y is the height of the surface from a mean line describing the surface, i. e., the centerline and x is the direction along this centerline or mid-plane. Table B-1 shows the CLA and RMS values for several mathematically described surface geometries.

There exist a number of recent papers and articles on surface definition, such as shown in References 32 and 33. These deserve further study, as do other works on this topic.

TABLE B-1 MATHEMATICAL SURFACE PROFILES

Profile	CLA	rms	rms CLA
<p>(1) Sine Wave</p> 	0.318	0.354	11.2%
<p>(2) Saw Tooth</p> 	0.25	0.289	15.6%
<p>(3) Parabola</p> 	0.256	0.298	16.3%
<p>(4) Parabola</p> 	0.256	0.298	16.3%
<p>(5) Step Function</p> 	0.5	0.5	0%
<p>(6) Gaussian Distribution of Surface Asperities</p>	$1.0\sigma^*$	0.796σ	25.8%

* σ = Standard deviation

3. LITERATURE REVIEW

A review of the existing literature and current work in the area of thermal contact conductance has shown that most of the reported work has been done in the presence of air as an interstitial fluid. Due to the recent requirements of nuclear fuel element heat transfer, a number of investigators have carried out experiments in gases other than air. This is especially true of reported European work during the past ten years.

The majority of all the work was of a sufficiently specialized nature to make this data difficult to use for generalized correlations. A second shortcoming was the absence of adequate information on the surfaces, their properties, and other test parameters. Since the area of major interest in the current work is that of joints in a vacuum, the emphasis in this survey will be in that area; however, for completeness as well as understanding, a sufficient amount of non-vacuum data discussion will be included.

In addition to the above, a fair amount of Russian material has recently become available on the heat transfer of machine element contacts and similar topics (Ref. 28).

No discussion of the thermal contact literature would be complete without giving due credit to Holm (Ref. 1), whose book presents a basis of approach utilized by most investigators. Although Holm's work was directed primarily toward electric contacts, sufficient similarity exists to apply many of the approaches provided in this reference. The reader is referred to pages 10 to 51 in Reference 1 for further details, although selected observations and comments from Holm will be made throughout this report.

The existing literature can be divided into studies of contacts in the presence of air and other gases and studies of contacts in vacuum. These will be considered separately. No distinction will be made between experimental and analytical study, except that the emphasis will be on the former. The latter are adequately covered in References 3, 5, and 9. It should also be noted that Reference 28 presents the most comprehensive bibliography on this topic. The reader is referred to these references for details not shown in this report.

3.1 CONTACTS IN AIR AND OTHER FLUIDS

Cetinkale and Fishenden (Ref. 9) carried out a theoretical and experimental study on contacts in air, spindle oil and glycerol. They assumed that the heat flow lines at some distance from the contact point between metallic rods are parallel to the rod axis as well as to each other. As the interface is approached, the flow lines converge toward the actual contact spots because the thermal conductivity of the solid is much greater than that of the interstitial fluid. They determined the temperature distribution near the interface by means of the relaxation method, assuming circular solid contact spots distributed uniformly and formed by cylindrical elements.

Steady state equations were developed for the interface thermal conductance on the basis of the above assumptions.

Conventional methods were used to define the fluid conductances for the interstitial gap. An expression for the case of a rarefied gas in the interstitial gap was written which uses a kinetic theory relation for the case where the mean free path of molecules is much greater than this finite gap; however, this expression was not used in their experimental work.

The ratio of the actual contact area to the total apparent contact area was shown to be a function of the ratio of apparent contact pressure to the Meyer hardness (the average resistance to indentation), which is approximately proportional to yield strength. This approach states that the softer of the mating materials will flow plastically until the mean solid spot pressure is equal to its Meyer hardness.

Cetinkale and Fishenden (Ref. 9) were able to match theory and experimental results for ground surfaces only in tests with steel, brass and aluminum contacts with air, spindle oil or glycerol as the interstitial fluid. For other surface finishes, constants in their theoretical equations have to be determined experimentally for each such case.

Weills and Ryder (Ref. 10) performed a primarily experimental investigation of dry air and oil filled metallic joints of 7.62 cm diameter x 7.62 cm long aluminum steel and bronze over a range of temperatures from 150 to 200°C and for pressures up to about 50×10^6 Newton/m². The authors utilized the constriction resistance

approach of Holm (Ref. 1) to explain some of the observed results. Heating was accomplished using an induction heated copper block, and heat flow was evaluated by measurement of the cooling water temperature rise. Thus, measuring the temperature gradient provided knowledge of thermal conductivity of the sample cylinders. Some observations made in Reference 10 are shown below.

Copper plating a steel surface increased the conductance by nearly a factor of 2. A similar increase was shown for oil filled joints over dry joints. The thermal conductance for steel (4140) increased linearly with pressure, whereas that for aluminum and bronze increased exponentially. A hysteresis loop is formed when the contact pressure is decreased following an increase. The decreasing pressure conductance values always were higher. Surface roughness values are given for the samples in this reference, as are material composition and mechanical properties.

Brunot and Buckland (Ref. 11) presented data on the contact conductance of laminated steel joints with and without shims of steel, aluminum, or aluminum foil. Solid test blocks also were used. The laminations were parallel to the heat flow path. The results indicated that, in general, the coarser the finish, the lower the conductance, with the notable exceptions that rusted surfaces had lower conductances than clean surfaces. Another interesting observation was that parallel lay or laminations gave higher conductances than did perpendicular lay surfaces or laminations. The effect of shim materials indicated that for laminated surfaces aluminum foil, aluminum shim, steel shim (in that order) gave decreasing conductances except that any one of the shims was better than a bare joint.

Kouwenhoven and Potter (Ref. 12) present experimental data for metallic joints tested in air and in argon. Contact pressures ranged to 22×10^6 Newton/m², and average temperatures were approximately 90°C. One specimen interface in each pair had a surface finish of 7.6×10^{-6} cm (3 μ in.) whereas the other surface ranged up to approximately 10^{-3} cm (4150 μ in.) finish.

An interesting study was carried out on the deformation of ridges for a "ruled" surface (similar to a plowed field) having the shape of isosceles triangles. A relation for the area versus contact pressure is shown in equation and graphical form, but no experimental verification was made.

Barzelay et. al (Ref. 13, 14, 15, and 16) performed a large number of experiments in air, consisting of column apparatus tests as well as tests on a stringer joined to a skin surface. Materials investigated (Ref. 13 and 14) were aluminum (75S-T6) and 416 stainless steel, for the bare metals as well as zinc-chromate coated interfaces, aluminum, brass and asbestos shims and bonded joints. Test samples in the column apparatus were 7.62 cm in diameter and 2.54 cm thick (3 in. x 1 in.). Surface finishes ranged from 15×10^{-6} cm (6μ in.) to 300×10^{-6} cm (120μ in.) rms. Contact pressure was held constant at 48×10^3 Newton/m² (7 psi). The effects of heat flow, temperature drop, interface temperature and surface condition were investigated.

Barzelay et. al. (Ref. 14) reports an extension of previous work to include the effects of contact pressure, which ranged from 35 to 3000×10^3 Newton/m² (5 - 425 psi) for interface average temperatures of 93 to 204°C (200 to 400°F). It was noted that surface finish alone was not the dominant parameter in the determination of thermal conductance. Overall flatness or flatness deviation has a more dominant role in this respect. In a number of tests it was found that warping influenced thermal conductance to a greater extent than did either roughness or initial flatness.

An interesting observation made in this reference is the directional heat flow effects on the conductance value for a stainless steel-aluminum joint where the heat flow in the aluminum-to-steel direction was several times that for the steel-to-aluminum direction for otherwise unchanged conditions.

In References 15 and 16, Barzelay et. al., report results of thermal transient tests for a large number of stringer-skin combinations. These tests were directed toward needs for transient thermal performance of riveted aircraft joints. Considerable scatter of data was observed not only from sample to sample but also from test to test. This was particularly true for thin skin-stringer test samples. It was observed that while different configurations had the same initial conductance value, unequal heating caused distortions, which in turn resulted in a change of contact and conductance. Thus, joint geometry may cause variations in the conductance value during heating of composite aircraft-type joints.

Held (Ref. 31) investigated the heat transfer between machined and polished surfaces of steel and proposed a theoretical relation based in part on the work of Holm (Ref. 1).

Experiments were carried out on cylindrical samples where the same specimen was first lapped, polished, turned, planed, and scored, with conductance tests taking place between successive machining of these surfaces.

Held considers macroscopically plane surfaces; when these surfaces are pressed together they touched each other in at least 3 contact areas. The number of contact areas increases with an increase in pressure. The Hertz equation of elastic deformation of spherical surfaces are utilized in the analysis, where one such contact area is considered initially and the number of such contact points is considered independent of the load. Held considers elastic as well as plastic deformation, where plastic deformation is evidenced by the hysteresis effects observed.

Held proposes a theoretical expression of the form:

$$h_c = f(P) \quad (11)$$

which, in the elastic region at least, can be presented in the form:

$$h_c = B(P)^\beta, \quad (12)$$

where B and β are functions of the material and surface properties. Held was able to correlate experimental results and theoretical assumptions.

Laming (Ref. 17) performed joint conductance experiments for very coarse finish surfaces of brass, steel and aluminum in air, water and glycerol for contact pressures of $130 - 4800 \times 10^3$ Newton/m² (20 - 700 psi). A high load test at pressures up to approximately 80×10^6 Newton/m² (11,400 psi) was also performed in air for a steel-brass joint.

Laming proposed a semi-empirical approach based upon a "simple conductance theory" where the total conductance is made up of the solid and the fluid conductance. An expression for the fluid conductance is given which is based on a gap parameter only. Laming was then able to show that log-log plots of the solid conductance at high loads versus load were straight lines having a slope greater than 1/2. This solid conductance was obtained by subtracting the fluid conductance from the total conductance. At very high loads a constriction alleviation factor is introduced to account for the increased slope at high loads. Surface finishes for Lamings tests were 43×10^{-6} m to 61×10^{-6} m peak-to-mean surface distance, which represents a very coarse finish.

Fenech and Rohsenow (Ref. 2) reported a highly theoretical analysis of the thermal contact conductance problem. A cylindrical model was considered, where a cylindrical contact was surrounded by a coaxial heat-flow channel. Radial conductance is neglected as are radiation and free convection in the fluid surrounding the cylindrical contacts. The heat conduction equation for this model was solved by making justified approximations and by using average boundary conditions. A complex expression results which can be considered the sum of two fractions. The first fraction represents the heat flow in the voids and the second fraction, which is much simpler, represents the heat flow through the metallic contact. The latter would be the case for contacts in a vacuum.

In order to evaluate the geometrical properties and parameters necessary to solve the derived equations, a graphical method is proposed which utilizes recorded profiles perpendicular to each other for each of the contact surfaces. The corresponding profiles are then superimposed to determine the number of contact points, void thickness, and area of contact as a function of load, which is represented by different degrees of superposition of the profiles. Knoop hardness of the softer of the mating surfaces is required, to relate the apparent pressure to the contact area. Experimental results of an aluminum-Armco iron contact gave good agreement with this theory. Other tests were performed with machined pyramids of stainless steel against optically flat stainless steel and machined iron pyramids against optically flat aluminum. One set of tests was performed with solid cylinders with a neck machined to represent one solid contact spot of cylindrical shape. Reasonable agreement between theory and experiment was observed for the last series of tests with mercury, air, and water as the fluid surrounding the contact model cylinder.

A considerable number of other investigations, theoretical as well as experimental, are reported in the literature for tests in other than vacuum. A large body of such literature originated in the nuclear-energy field. The Russian literature indicates a considerable amount of thermal contact work, some of which is included in Reference 28, which was an outgrowth of this study.

3.2 CONTACTS IN VACUUM

The earliest reported work on thermal contacts in a vacuum was carried out by Jacobs and Starr (Ref. 18) for polished gold, silver and copper contacts at moderate contact pressures to 250×10^3 Newton/m² (36 psi). Tests were performed at 77K and at 298K; however, only the latter tests are of interest here. It was found that the conductance for copper varied linearly with load, whereas that for gold and silver varied as the 1/3 power of the contact pressure. Effects of dust and oil films also were discussed.

Boeschoeten and Van Der Held (Ref. 19) carried out experiments on aluminum-aluminum, aluminum-steel and aluminum-uranium joints at gas pressures varying from 130 to 10^5 Newton/m² (1 mm to 750 mm Hg) for air, helium, and hydrogen. The lowest of these pressures is still too high to provide useful data for vacuum conditions, however qualitative observations are of interest. These observations indicated that contact pressure has not much influence on the size of the contact spots but that their number varies proportionately with the contact pressure. They also stated the size of the contact spot was not greatly affected by the metallic joint material, thus providing a means to predict the conductance of metallic joints.

Of considerable interest is comparative data on Aluminum versus Aluminum joints provided by Boeschoten and Van Der Held (Ref. 19). They gave experimental conductance data for 10^5 Newton/m² (1 kgf/cm²) contact pressure, for different gases at atmospheric pressure.

Air	0.36 Watts/cm ² °C
Helium	0.95 Watts/cm ² °C
Hydrogen	1.38 Watts/cm ² °C
Silicon oil	1.9 Watts/cm ² °C
Glycerol	3.8 Watts/cm ² °C

The surface finishes were approximately 10×10^{-6} m, while 15×10^{-6} m was considered the average gap thickness. The vacuum test results of this reference were taken at vacuum pump pressures of 10^{-2} mm Hg (1.33 Newton/m²) which is not quite adequate for reliable vacuum data but provides useful trend data.

A perusal of Sanderson's (Ref. 23) data shows the effect of apparent interface gas pressure on the contact conductance of a uranium-Magnox interface joint. For helium, the pressure dependence ceases at 1000 mm Hg (1.33×10^5 Newton/m²). Below that gas pressure, the contact resistance increases about 8 fold as the gas pressure is reduced for tests at 200°C at contact pressures of 100 psi (689×10^3 Newton/m²). This is also indicated by separate thermal conductivity data for helium gas where the conductivity became constant at about 1100 mm Hg (1.46×10^5 Newton/m²).

For a similar joint in argon under the same conditions, the contact resistance at 1200 mm Hg (1.6×10^5 Newton/m²) was much higher than for helium, however, the value of contact resistance at near zero gas pressure was the same for both cases. The much higher resistance for the argon joint, about 1/2 of that at zero pressure, is notably different from helium data where it is 1/7 of the zero gas pressure value. This is not in conformance with the approximate 7 times higher thermal conductivity of helium over argon, and can lead one to conclude that some form of surface effects must have occurred on the metal surface. The fact that at zero gas pressure the thermal resistances were the same tends to support this view.

Wheeler (Ref. 20) proposed an interesting approach toward correlating existing data in vacuum. He plotted the contact conductances versus joint pressure divided by yield strength and was able to show a reasonable curve through the data points. For dissimilar materials, he used the yield strength of the softer of the mating materials. The slope of a line through the points is approximately 2/3. It is of interest to note that Aron (Ref. 27) could show that the data of Fried (Ref. 4) fell on this curve which he described by the expression $h = B (P/Y_0)^{2/3}$, where B is a constant and Y_0 is the yield strength of the softer of the two materials.

Ascoli and Germagnoli (Ref. 21 and 22) also report vacuum results for nuclear fuel-element cladding interfaces in vacuum.

Bory and Cordier (Ref. 23) report vacuum tests for steel-brass joints; however, only qualitative observations on the effects of initial and subsequent compressions and recompressions are given. Effects of elastic and plastic deformation and recovery are discussed. This work is important, but came too late to be studied in detail for this report.

Fried and Costello (Ref. 4) presented results of tests performed on aluminum and magnesium joints consisting of flat plates 3.2-mm thick. Surface finishes ranged from 15 to 185×10^{-6} cm (rms) and contact pressure ranged up to 240×10^3 Newton/m² (35 psi). Tests were run in a vacuum of 0.013 Newton/m² (10^{-4} mm Hg) or lower.

It was reported that flatness deviation had a large effect on contact resistance. While finer surface finishes resulted in higher conductance values, flatness deviation could affect results regardless of surface finish. It was also found that introduction of a softer shim material improved the conductance of joints and was particularly useful for joints having high flatness deviations.

Later work by Fried (Ref. 24) gave test results for silicone grease and silicone rubber joint fillers. High vacuum silicone grease was found to be extremely useful in improving the thermal contact conductance in vacuum tests of metallic joints. This was also observed by Clausing (Ref. 3).

An attempt was made to obtain a semi-empirical correlation of vacuum test contact conductance data based on an approach suggested by Held (Ref. 31) and Laming (Ref. 17). The results of this attempt were inconclusive due to a lack of sufficient data. Reference 24 also discusses available references on vacuum experiments.

Jansson (Ref. 25) reports results of aluminum joints and beryllium joints in vacuum. These tests provided no specific information relating surface finish to conductance. Only ranges of values were obtainable for a given material and load. It was observed that outgassing of surfaces prior to tests resulted in higher conductances at low loads.

Tests were performed on $2.54 \times 2.54 \times 0.64$ cm ($1 \times 1 \times 1/4$ inch) test specimen in a fairly simple test fixture.

Jansson also reports data on interface fillers of epoxy cement, gold foil, aluminum foil, lead foil and indium foil. Indium foil was found to give the highest conductance improvement, followed by epoxy cement, lead, aluminum and gold in that order.

In addition to the work reported in this Document, the most extensive contact conductance investigation in a vacuum is that reported by Clausing and Chao (Ref. 3). These

investigators utilized a column-type apparatus of careful thermal design to provide careful test data. Clausing performed tests on 2024 Aluminum, AZ31 Magnesium, 303 Stainless Steel and Brass. Contact pressures ranged to 7000×10^3 Newton/m² (approximately 1000 psi). One test was performed using silicone grease in the joint, otherwise the joints were run dry.

Clausing presents a theoretical model which considers microscopic constriction resistance and a macroscopic constriction resistance. The normal contact area is divided into contact and non-contact regions. The latter, by definition, is the part of the interface containing a negligible number of microscopic contacts. The contact region, defined as the macroscopic contact area, is populated by a high density of microscopic contact areas.

This model was shown to permit prediction of Clausing's experimental data and it apparently permits explanation of previously puzzling results. The value of this work lies in the proposed approach which recognizes the dominance of the macroscopic constriction effects, although it requires further effort to make it more generally applicable.

Due to schedule and time limitations, Clausing's model and correlation technique was not applied to the work presented in this report. It is planned to apply the Clausing model to present and subsequent work performed during the next contract period in order to test its adequacy for prediction of thermal contact conductance. One possible problem area may arise when more than one contact region exists, since the model is based on a spherical segment which assumes one contact region.

A considerable number of other experimental metallic joint studies in a vacuum are currently underway and are listed in the bibliography only, since they were received too late for discussion.

A recent memorandum by Holm (Ref. 7), has the stated objective of providing a simple rule for precalculations of the thermal conductance of metallic contacts when the load is known. In particular, this method is directed to space flight applications, i. e., vacuum conditions for "plate" contacts as defined in Reference 1.

Constriction resistance is defined in electrical and thermal terminology assuming similar property relations. The effect of alien films and their effect on thermal versus electrical resistance is discussed. Thermal radiation between the mating surfaces is considered as is gaseous conduction. Effects of reduced pressure also are considered.

The general approach to this problem is to utilize a curve of load versus electrical resistance from Reference 1 and by relying on the Lorentz-Wiedeman relation between electrical and thermal conductivity, to predict the thermal conductance of a joint. This curve proposed by Holm is one for copper, which is to be used for other materials by the ratio of hardness and thermal conductivity for the material of interest. Variables not considered are flatness deviation, surface finish and effects of plastic deformation.

This approach would be very appropriate if it did not require prior knowledge of the true contact area in order to be useful. However, in order for this relationship to be used for engineering calculations, one must assume this true contact area.

The major contribution of Reference 7, as based on the work of Holm in his pioneer book (Ref. 1), is to demonstrate a method of approach to a possible solution. In addition it should be stated that Holm makes a number of extremely valuable observations (Ref. 1 and 7) concerning surface films, deformation, and other effects.

4. PROPOSED MODEL

In order to develop a prediction method for metallic contact heat transfer in a vacuum, a realistic model has to be found to describe the phenomenon and to aid in the writing of the pertinent equations. Most of the existing models do not satisfactorily represent the thermal performance of a joint.

The model proposed by Clausing and Chao (Ref. 3) provides probably the most satisfactory approach to the problem on hand, although a certain number of refinements and modifications in the input data may be required.

The present investigators were independently working on an approach similar in nature to that proposed by Clausing and Chao during approximately the same time period. The investigator's model was somewhat simpler in that a spherical contact against a flat plate was considered to represent 1) the asperities individually and 2) the cumulative effect of a group of asperities on an elastic substrate. Thus, (1) would represent Clausing's microscopic and (2) his macroscopic contacts although no distinction was made between them since it was assumed that a parameter to be determined for each type of contact problem would account for the initial ratio of contact and non-contact regions.

The Hertz equation of elastic deformation for spherical contacts was considered to be applicable for the problem on hand and was discussed by Holm (Ref. 1) and Held (Ref. 31) sometime ago and concurrently with this work by Clausing (Ref. 3). In particular it should apply after the initial contact has been made during which a number of asperities have been plastically deformed. This initial effect must still be determined experimentally.

The theoretical treatment will not be presented here since it is available in the literature and discussed in particular by Archard (Ref. 26). It is shown that the true contact area is a function of the load, if the deformation is truly elastic, resulting in an expression of the form

$$A = BP^m, \quad (13)$$

where B is a parameter depending on the local radius of curvature and the elastic constants of the material. The power m is $2/3$ for the ideal case, and higher than this for the case of many small protuberances in elastic contact. Values approaching unity have been shown to be reasonable. (See Appendix A.)

In order to study this problem in greater detail, an experimental program of experimentally finding the area change with load was carried out by Atkins at MSFC-NASA to complement the thermal test program. The three models chosen to represent the problem at hand were a cone, ellipse and hemisphere; these were placed between two flat steel plates and subjected to increasing loads. For each such load setting, a piece of pressure-sensitive paper was inserted in order to determine the new contact area after plastic deformation. The results of such a deformation model test are shown in Figure 4-1.

It should be noted that the foregoing model appears to represent part of the physical picture of the contact heat transfer regime for metal-to-metal joints. The apparent difference of approach between investigators is not whether the elastic deformation model of Hertz is valid; there seems to be agreement on this. The problem is one of defining the way in which this model is to be used for the prediction of the thermal contact conductance. This investigator believes that a semi-empirical approach combined with back-up analysis is the best way to attack the problem since the exponents and parameters of equations 11, 12 and 13 are functions of the surface properties which are difficult to define presently. This approach will be checked against existing thermal test data which at present is meager for vacuum tests, but should be ample by the time the next summary report on this subject will appear.

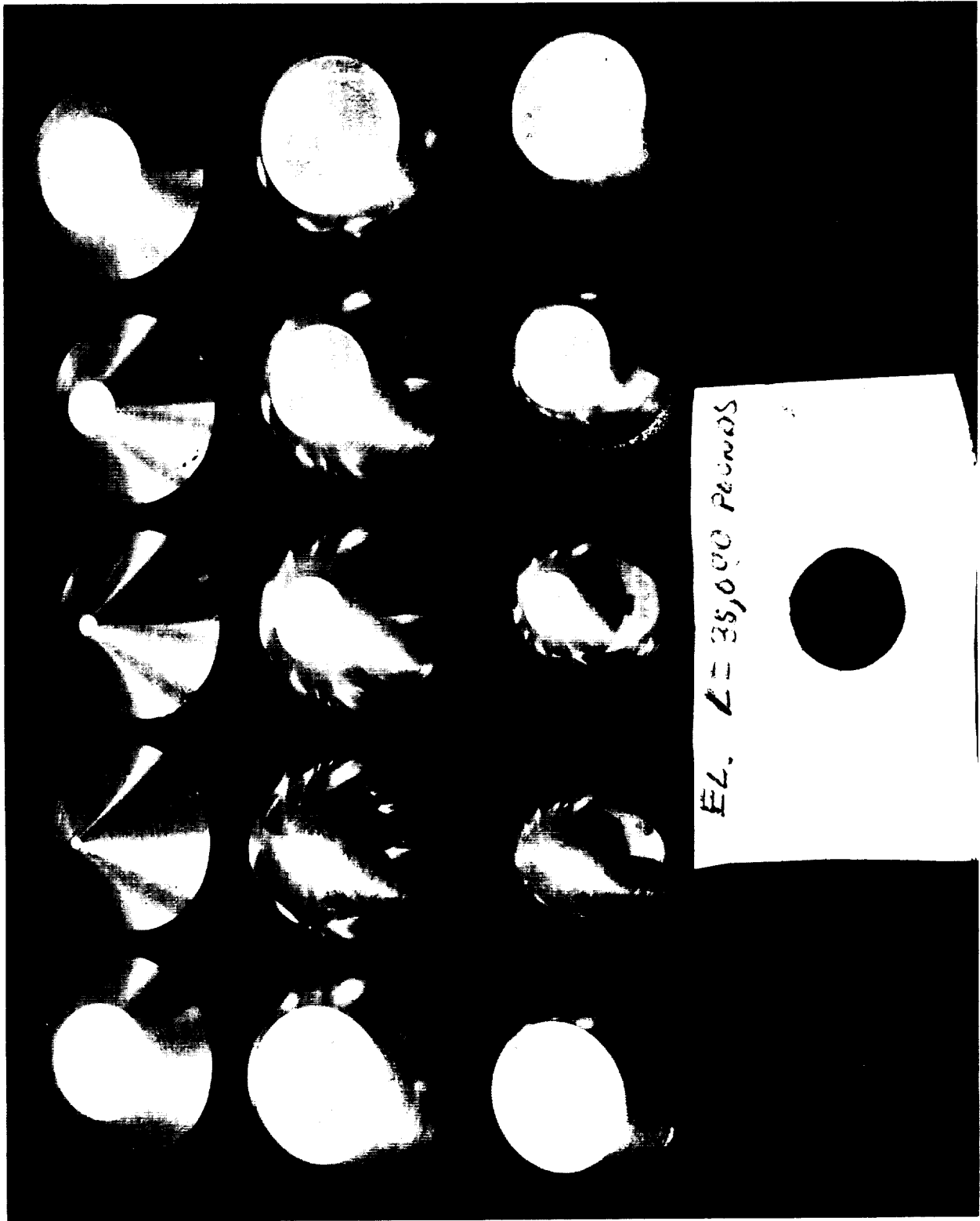


Figure 4-1. Deformation Test Model

5. EXPERIMENTAL PROGRAM

5.1 OBJECTIVES

A study of the problems in the early stages of the thermal contact conductance work, has indicated a need for experiments to do the following: 1) Aid in the understanding of the heat transfer mechanism; 2) Provide data to verify existing analyses; and 3) Provide data to aid in the development of new analytical methods.

To this end a thermal contact conductance apparatus suitable for use in vacuum was developed which would permit accurate measurement of thermal conductance as a function of contact pressure. As opposed to the flat plate apparatus used in the investigations reported in References 4 and 5 by the principal investigator of this study, this apparatus utilized cylindrical columns to minimize flatness deviation and constriction resistance effects due to the sample size.

5.2 TEST APPARATUS

A schematic view of the test apparatus is shown in Figure 5-1 and a photograph in Figure 5-2. Figures 5-3 and 5-4 show the heat flow section of the apparatus with a specimen in place, with and without the radiation shield.

The samples consisted of two metallic cylinders having a diameter of 5.08 cm and a length of 7.62 cm each. Each sample was instrumented with four copper-constantan thermocouples to determine the axial temperature gradient due to the uniform heat flux passing between the electric heater and the liquid cooled sink.

Contact pressure could be varied by means of a stainless-steel bellows which was pressurized in accordance with the desired load. The load was measured using a strain gage load washer on the heat sink side (See Figure 5-1).

The entire assembly was installed in a bell-jar vacuum system with a right-angle cold trap utilizing a 4-inch oil diffusion pump preceded by a roughing pump to achieve a vacuum of 10^{-4} mm Hg (1.33×10^{-2} Newton/m²) or better.

The details of the apparatus are described in the following sections.

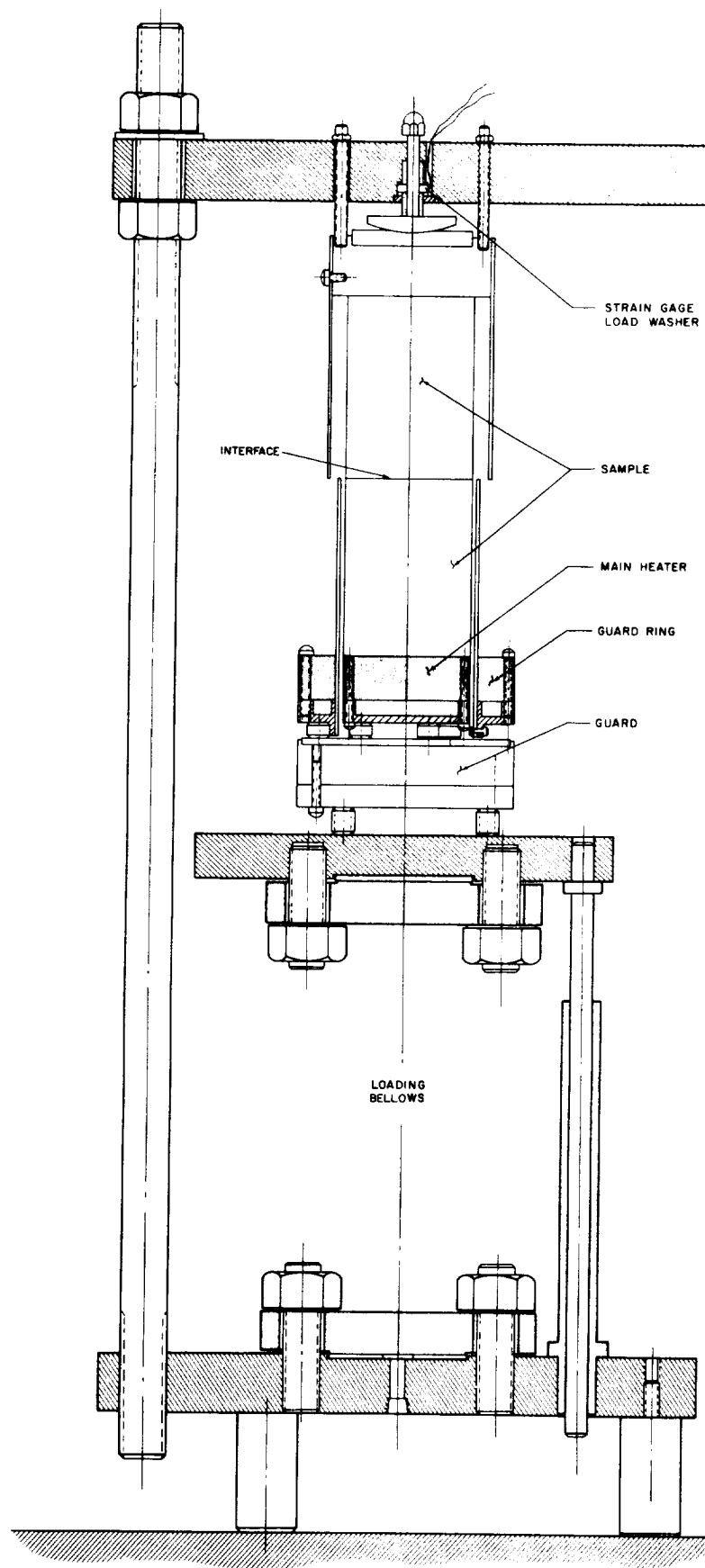


Figure 5-1. Thermal Test Apparatus Schematic

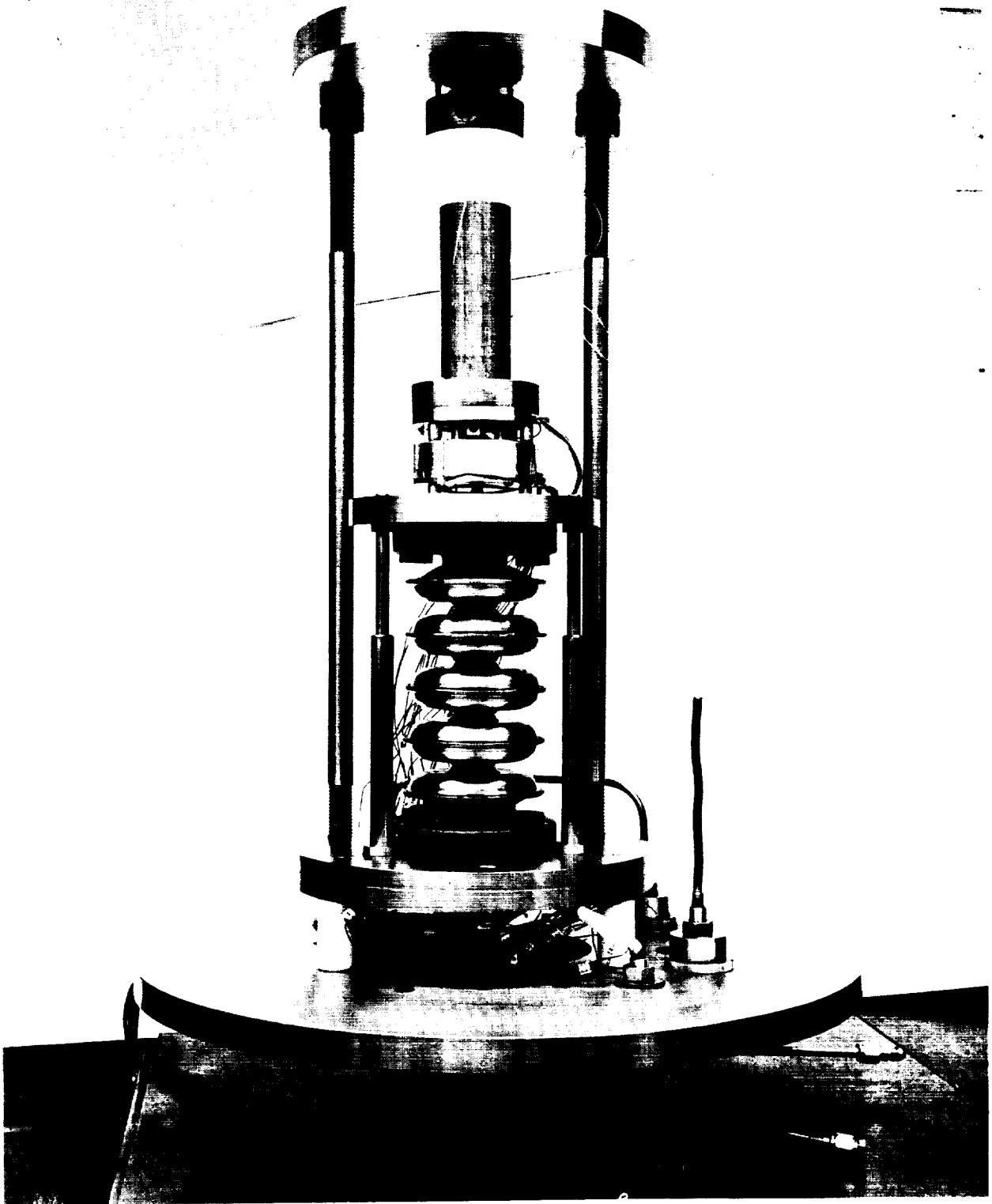


Figure 5-2. Thermal Test Apparatus During Construction

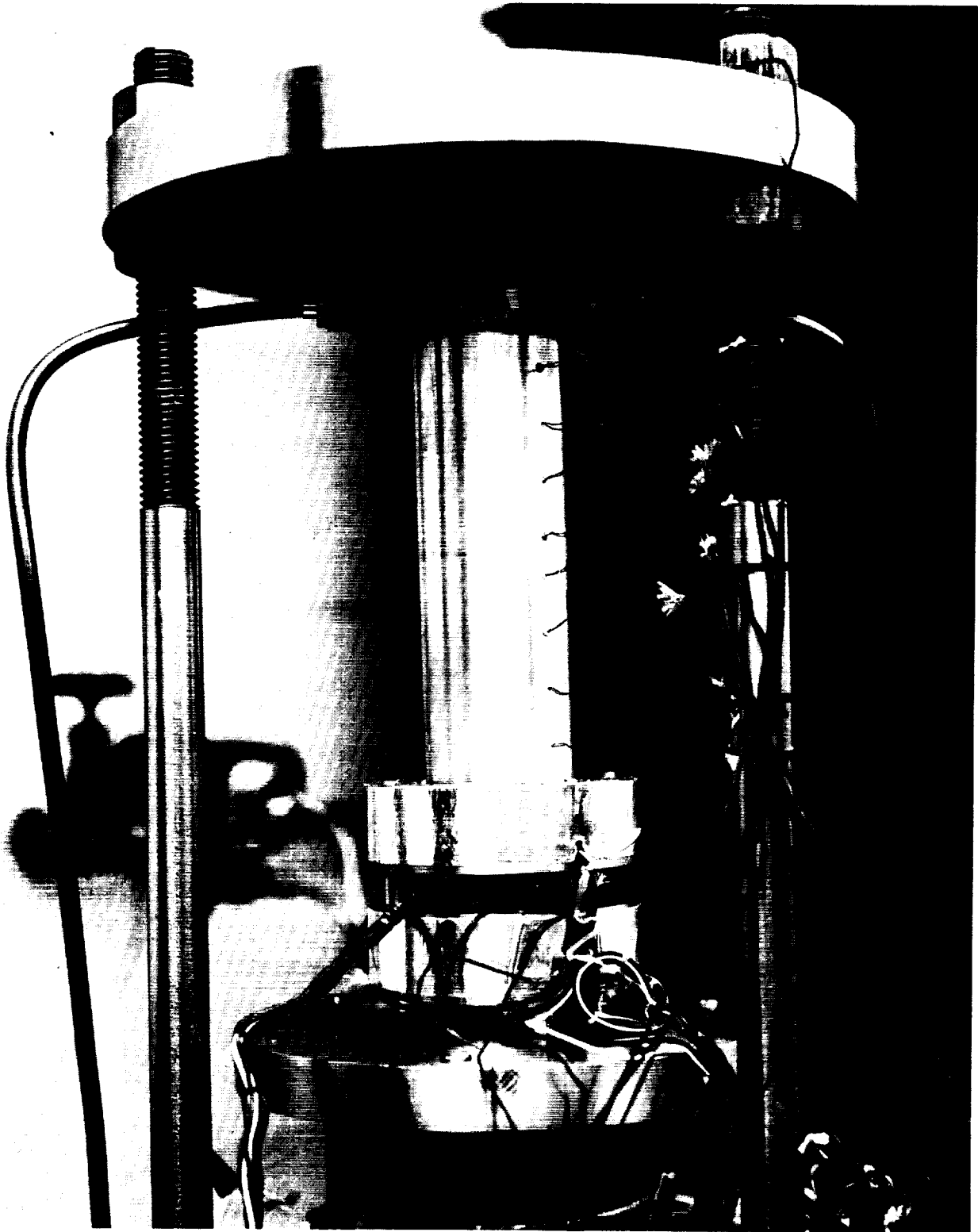


Figure 5-3. Thermal Conductance Apparatus with Sample

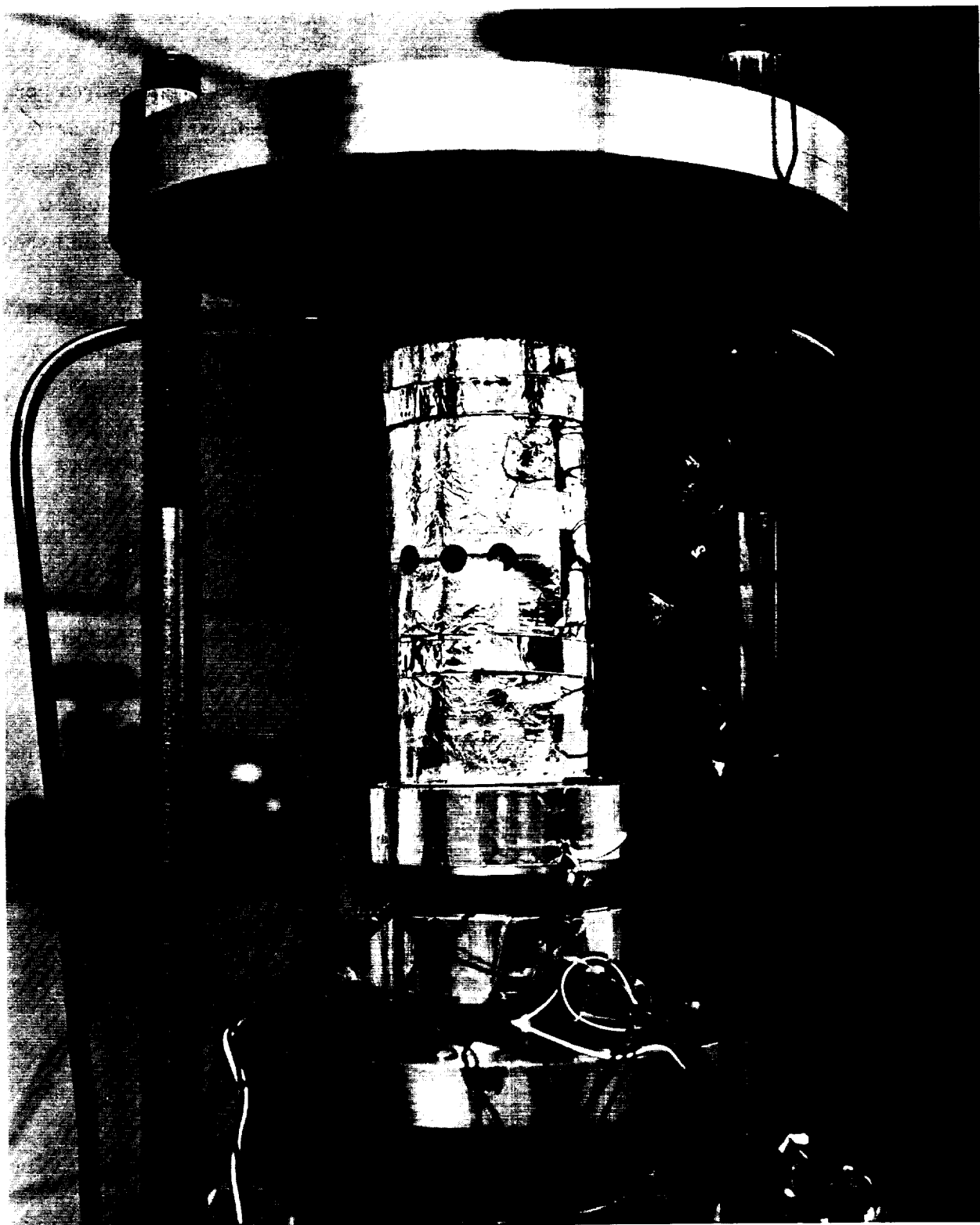


Figure 5-4. Thermal Conductance Apparatus with Sample and Radiation Shield

5.3 LOADING OF SAMPLES

During the early stages of the program it became apparent that contact pressures considerably higher than the planned 3.4×10^5 Newton/m² were required to obtain satisfactory understanding of the thermal contact conductance mechanism. Evidence obtained by other investigators supported this requirement. For this reason, the new loading (pressure producing) system was designed to handle contact pressures in excess of 7×10^6 Newton/m² by means of a pressurized bellows loading mechanism. A vacuum-tight stainless-steel bellows was pressurized externally with dry nitrogen thus exerting a load on the test specimen in accordance with the regulated nitrogen supply pressure. (See Figure 5-1). One of the most desirable features of this system is the ability to vary the contact pressure while the samples are under vacuum. An additional feature of this system is the ability to keep the interface surfaces separated during pump-down, thus aiding in their outgassing rate.

Earlier tests reported in References 4 and 24 had utilized calibrations based on the nitrogen pressure in the loading bellows as a means for measuring the contact pressure. This method has the shortcoming of requiring careful manipulation to avoid hysteresis effects. In order to simplify the system and to increase the accuracy of the data, a strain gage instrumented load washer* was installed in the apparatus as shown in Figure 5-1. This permits a continuous monitoring of contact pressure independent of any form of residual effects. A spare load washer was used for temperature compensation.

Prior to starting the first test, the load measuring assembly was calibrated using an Instron loading device to obtain a curve of strain gage reading versus load. This and a test performed at the conclusion of the program indicated that contact pressure readings below 340×10^3 Newton/m² (50 psi) are subject to an uncertainty of $\pm 10\%$ or less; contact pressures higher than that were reproducible with an accuracy of better than $\pm 1\%$.

5.4 CALORIMETRY

The heat source utilized in this test was a 100-watt electric resistance element embedded in the mainheater assembly, which is guarded by a ring heater and a rear

*Lockheed Electronics - WR-7-3

guard heater as shown in Figure 5-5. This system is arranged in a manner such that no temperature difference exists between the mainheater and the guards (each of which is separately controlled) so that all thermal energy from the mainheater has only one direction to go: into the test sample. In order to monitor this system, thermocouples were fastened to several surfaces which "see" each other.

Minimum cross sectional area supports, made of tubes (See Figure 5-1) were used between the rear guard and the mainheater in order to minimize heat leak errors, even though the facing surfaces were kept at nearly the same temperature. The desired range of temperature differences between potential heat-leak points were kept at ΔT 's of 1°C or less in order not to exceed $1/2$ of 1% heat flow errors. Initially these temperature differences were controlled by use of a deviation amplifier, but experience indicated that manual control, with proper judgment, resulted in less time delay between steady state points. Future tests will, however, be tried with other than manual control.

The allowable temperature differences were dictated by the amount of heat passing through the test sample, since high heat fluxes through the sample permitted higher heat losses from the heater without increasing percentage losses and errors.

In order to minimize heat losses by radiation from the sample to its surroundings, a cylindrical aluminum guard sleeve was wound with 2 sets of heater wires (See Figure 5-6.). Experience in preliminary tests demonstrated extreme difficulties in matching the temperature gradient of the sample in the "sleeve" guard. In fact it was found that the guard sleeve could introduce errors if improperly adjusted. Because of the disproportionate amount of time required to adjust this guard sleeve and due to possible errors, a new guard consisting of an aluminum foil covered piece of paper was made into a sleeve and used as a guard. Thermocouples were attached at several places to check the ΔT between the guard and sample. Calculations indicated that a 5°C difference between sleeve and sample would result in errors not exceeding $1/2$ of 1% for nearly all runs depending on heat flux. Measurement indicated that the ΔT 's were not in excess of this value for low heat flux rates and slightly higher at higher heat fluxes, keeping such errors well below allowable limits. The peripheral holes in the sleeve were cut to permit observation of the sample alignment when the vacuum system was closed. The errors due to these penetrations are negligible.

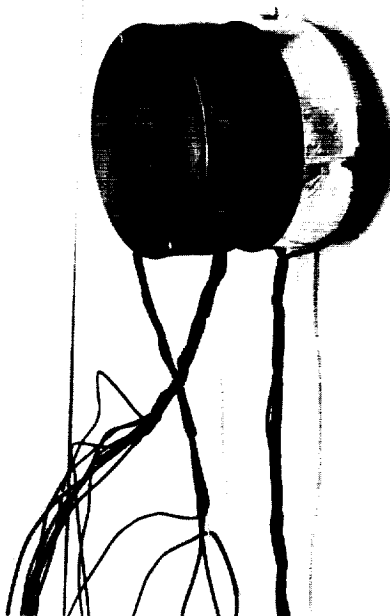
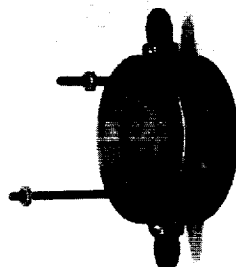


Figure 5-5. Heater, Guard Heaters, Heatsink, and Load Button

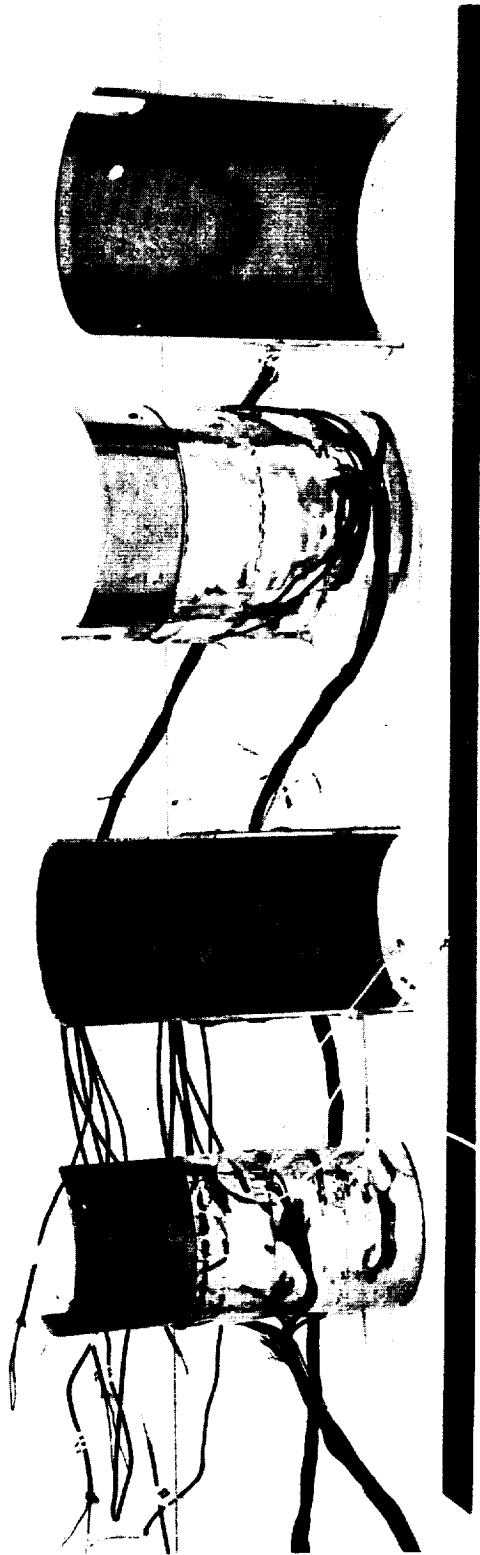


Figure 5-6. Radiation Guard Heaters

The basic procedure of measurement was as follows:

1. Set contact pressure and monitor this pressure.
2. Set main heater power input and monitor.
3. Adjust guard heaters to approach a minimum ΔT condition and repeat periodically until ΔT 's are within limits; read sample temperatures and all power inputs at 1/2-hour intervals for 3 readings. If temperature readings do not vary more than 0.2°C from other two values for same thermocouple, then accept reading. If not, continue until conditions are met.

The heat flux was determined by measuring the regulated d-c power input, i. e. , voltage and current using precision instruments. In addition to this, the hot-heater resistance was obtained by momentarily burning off the power. In order to eliminate leadline losses in the calculation, the ratio of heater winding resistance to total system resistance was measured and a correction applied to all readings. An ESI bridge having an accuracy of $\pm 0.05\%$ was used for these resistance measurements.

Voltages were measured using a Fluke differential voltmeter having an accuracy of $\pm 0.05\%$. The ammeter used had an accuracy of $\pm 0.5\%$ of full scale which meant errors of approximately 2% for the average range of currents. In order to provide a check on the quality of measurements, power input was computed by the relations EI , E^2/R , and I^2R . It was found that the EI value consistently fell between the other two methods by $\pm 3\%$ indicating that there existed a possibility of error in the hot resistance value, since E^2/R was consistently lower and I^2R consistently higher. If on the other hand the current measurements were high and resistances correct, then one would expect I^2R to be higher than EI . On the basis of best judgment, heat fluxes were computed on the basis of EI and corrected for lead losses, since this did not require the momentary interruption of power. Additional work on the adequacy of these measurements will continue.

A check was performed on the adequacy of the heat flow measurement by determining the thermal conductivity of a piece of Armco iron. The measured value came within 2% of the published Battelle data, which indicates that the data, considering all possible variables, is quite good. If only thermal conductivity measurements were performed, this accuracy could probably be improved. However, for conductance measurements, with their many sources of error, the cost of improving this system is not quite worth the effort at present. Subsequent work will probably require improvements.

5.5 TEMPERATURE MEASUREMENT

Considerable attention was paid to accurate temperature measurement techniques in order to minimize possible measurement errors, since the quality of the temperature measurement directly affected the quality of the interface thermal contact conductance obtained. Forty gage (7.6×10^{-5} m diameter) copper-constantan precision grade thermocouple wire was used to make the thermocouple junctions. This grade wire has a nominal tolerance of $\pm 0.3^\circ\text{C}$ over the range of interest, but was found to be considerably better by experience. Junctions were made by mercury-pool arc-welding techniques.

The thermocouples were installed in the test samples in 2.54-cm (1 inch) deep holes in order to place the junction at the cylinder axis (Figure 5-7). The junction was embedded with Eccobond 56C, an epoxy base cement having a thermal conductivity equal to that of stainless steel. Figure 5-8 shows the installation technique. In order to assure that the thermocouple bead actually contacted the sample at the cylinder centerline, a 0.325-cm diameter hole was drilled at the desired axial thermocouple location and a tube of the same material as the sample was inserted with the thermocouple installed. This method had the advantage that there was less likelihood of drill runout than if a small diameter drill had been used. It also permitted more positive installation and location of the thermocouple junction. The only exception to the matching of material was that an aluminum tube was used with the magnesium sample. This was not expected to result in an error, because 1) the thermocouple junction was in contact with the sample magnesium, and 2) the thermal effect of different material was not adverse because of the higher thermal conductivity of the aluminum. This would not result in a delay to reach thermal equilibrium.

The choice of 40-gauge thermocouple wire was dictated by the desire to minimize conduction losses. In spite of its small diameter, no adverse emf characteristics were observed in past experiences with several hundred couples from such wire purchased from Thermo-Electric Co. The question as to the proper response of the thermocouples as embedded in the samples when in a vacuum was circumvented by use of the Eccobond 56C, a fairly free flowing epoxy cement, which was inserted and packed around the thermocouple bead, metal sleeve, and wire. Thus the bead was hermetically isolated from the surrounding atmosphere.

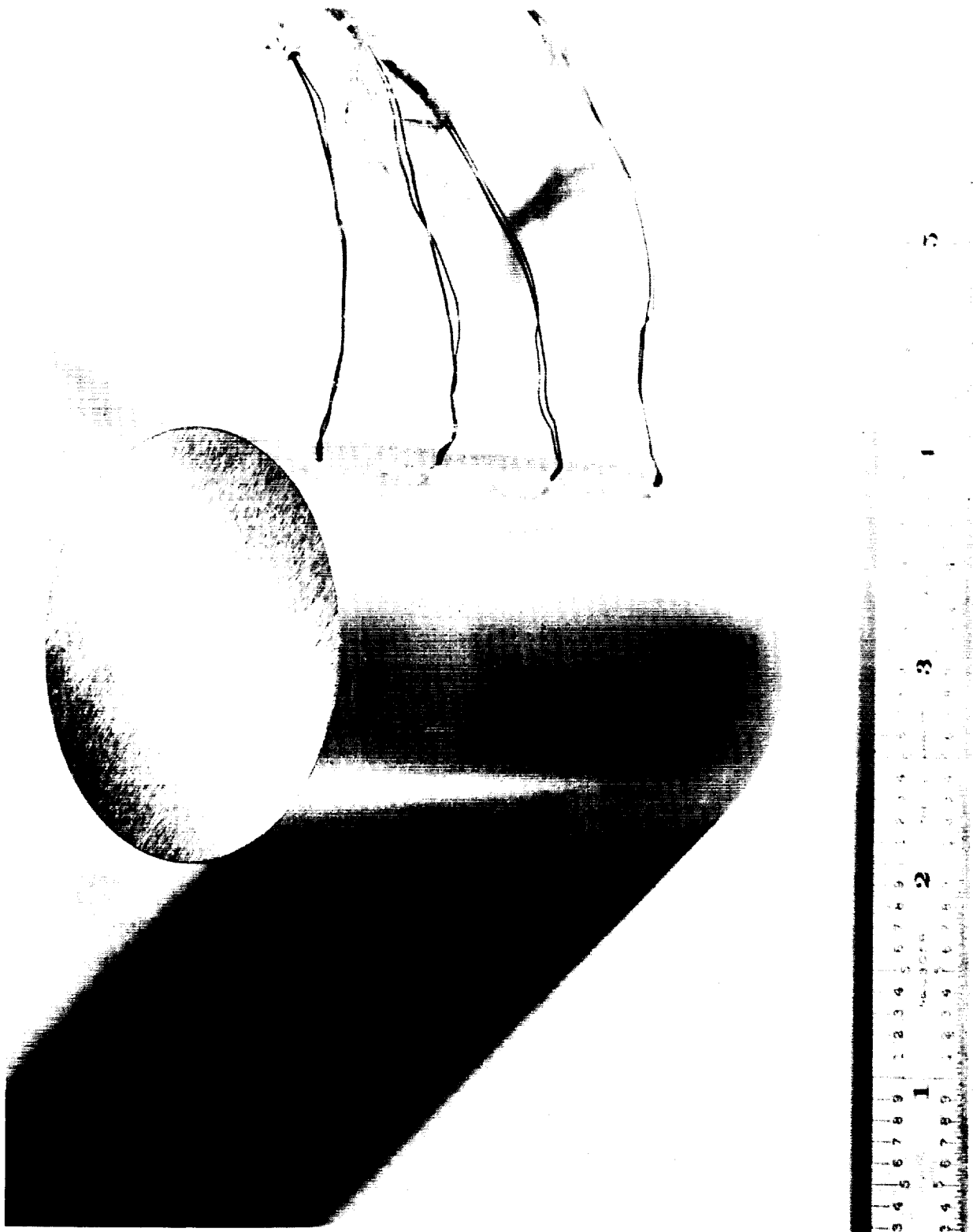


Figure 5-7. Test Sample with Thermocouples

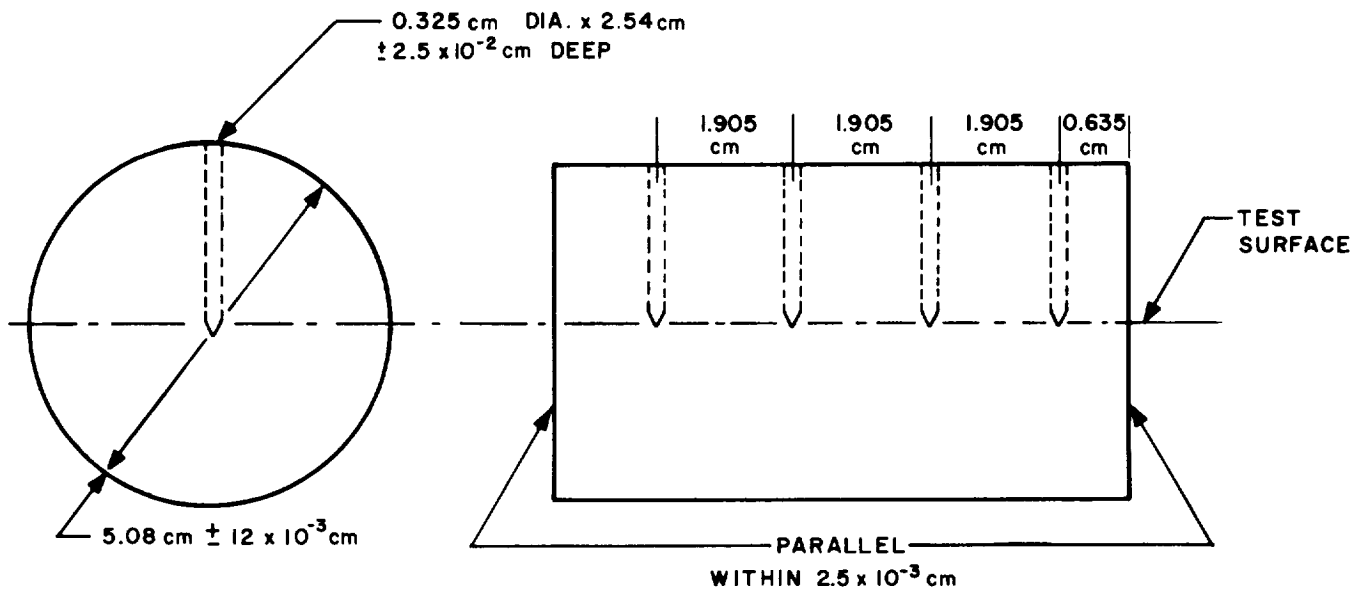


Figure 5-8. Thermocouple Installation Layout

In order to be assured of proper response of these thermocouples, they were placed in a constant temperature oven after being installed in the sample, and the consistency of the temperature readings was checked. Of more than 60 thermocouples tested, only 4 were found to require corrections in the computation of conductances for the range of temperatures of interest (25 - 50°C).

Initially it was planned to install thermocouples along sample axis and around the periphery at 120° intervals. Experiments, using surface thermocouples, indicated that the temperature difference between these couples was less than 0.1°C, when using the stainless steel specimen (i. e., low thermal conductivity material). This indicated that the temperature profile was essentially flat and led to the decision to omit other than axis thermocouples.

Thermocouples were installed in the specimen 0.635 cm (1/2 inch) from the interface and then spaced 1.905 cm (3/4 inch) apart for a total of 4 thermocouples per sample half. Particular attention was paid to the accuracy with which the axial distances between thermocouples were controlled, since the axial distance versus temperature

plots were used to project the temperature gradients to the interface and thus obtain the interface temperature difference.

The constriction resistance effects at and near the interfaces require that thermocouples be located in the undisturbed region in order to correctly project the temperature gradient. Since only the sample test interfaces are of interest, the heat source and heat sink interfaces with the samples had high vacuum silicone grease applied as a heat transfer promoting device. Thus no significant constriction effects were caused at these interfaces.

The temperature difference ΔT shown in equation 1 is based on the experimentally obtained temperatures, which are then extrapolated to the interface. The accuracy with which this ΔT can be obtained is a function of the accuracy with which the temperature gradient in the sample can be obtained. For high values of contact conductances the ΔT usually was quite low. Conversely, for low values of conductance the ΔT was high. Since a high ΔT resulted in a higher percent accuracy, the relative percent accuracy of contact resistance obtained was constant. A representative gradient curve is shown in Figure 5-9.

Of the thermocouples used in the sample each had its own cold junction. Their emf was read on a Leeds and Northrup K-3 potentiometer, with individual couples switched by means of a transfer switch. Figure 5-10 shows the vacuum system, thermocouple recorder, power supply, instrument panel, galvanometer and standard cell.

5.6 SAMPLE PREPARATION

The test samples were prepared from the same batch of material for each metal. The materials used were:

- 6061-T-6 Aluminum
- AZ-31B Magnesium
- 304 Stainless Steel
- OFHC Copper (99.96% purity)
- 2024-T-4 Aluminum (these samples were not tested in this program).

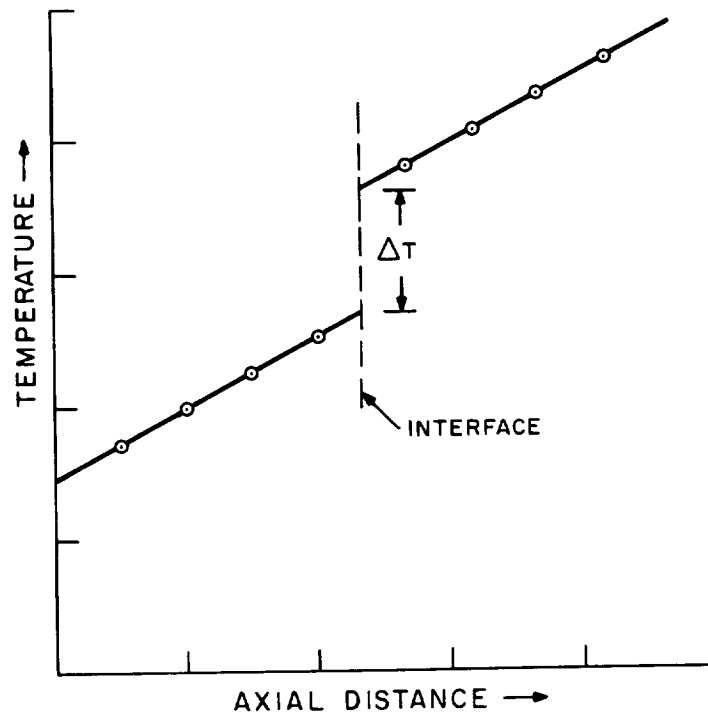


Figure 5-9. Representative Temperature Gradient Curve

All samples were made from round bar stock larger in diameter than the desired 50.8 mm diameter and turned to size and length to tolerances of $\pm 13 \times 10^{-3}$ cm on diameter and thermocouple hole location. End surfaces were finished to approximately 1.3×10^{-6} meter (rms) on the end surfaces not subjected to test. The other ends were finished as required.

For manufacturing purposes, surface finishes were checked with a Physicist Research Co. Profilometer Amplimeter Type 11Q, a tool crib quality instrument. Subsequent measurements with a "Talysurf" profilometer are discussed later.

Table 5-1 shows the sample materials, sample number, and other pertinent properties and information. All samples were subjected to a Rockwell hardness test on the machined surface not used for the test interface. This was done in order not to damage this interface test surface. The readings, which should be the same on both ends of the cylindrical sample, are shown in Table 5-1.

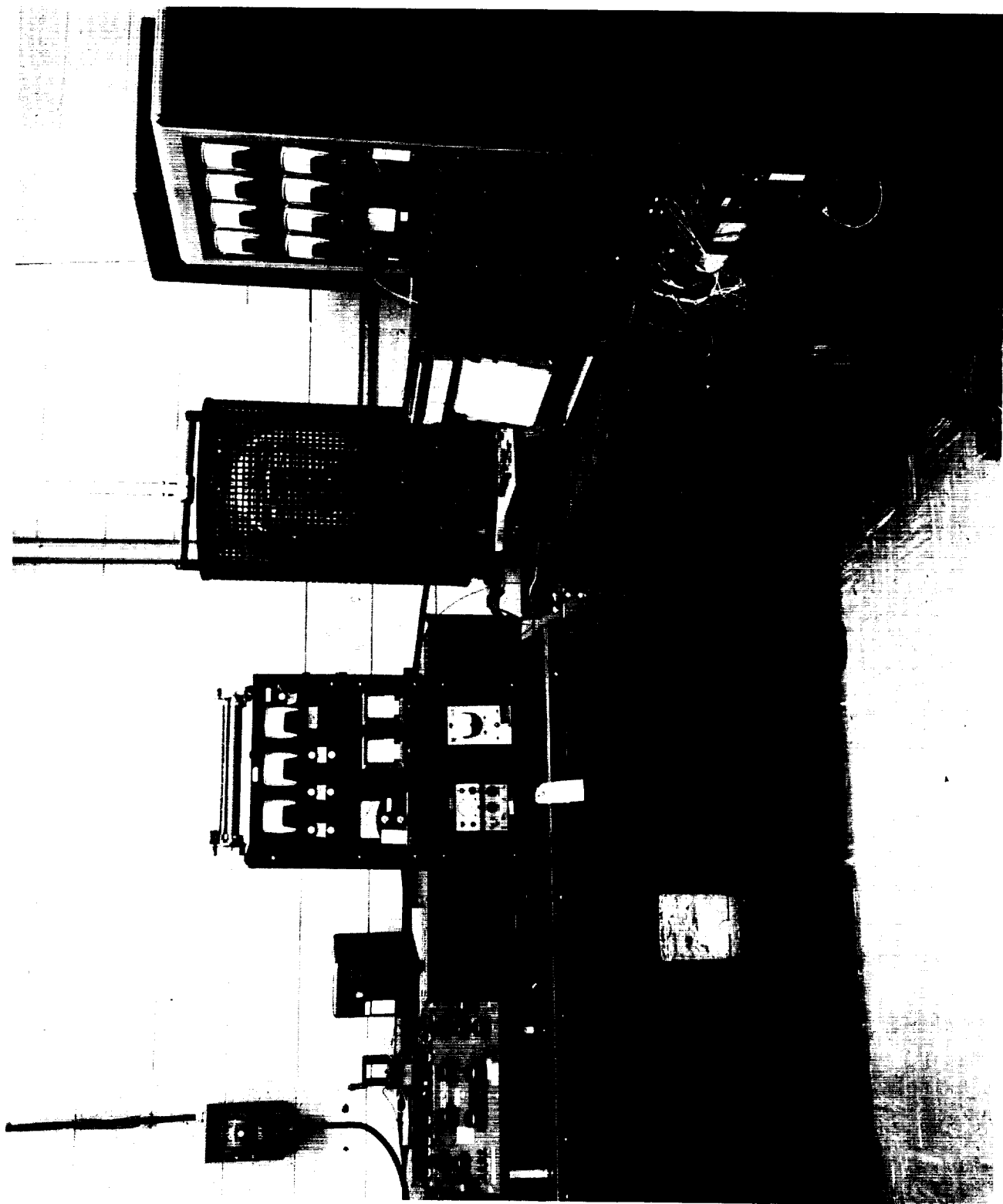


Figure 5-10. Vacuum System and Test Area

Sample Number	Material	Surfa	
		(RMS)	
		micro-meter	micro-in
1	Stainless Steel 304	0.38	15-15
2	Stainless Steel 304	0.25	10-10
3	Stainless Steel 304	1.3	42-60
4	Stainless Steel 304	1.1	43-48
5&6	Not Tested.		
7	AZ-31B Magnesium	0.30	8-16
8	AZ-31B Magnesium	0.30	8-16
9	AZ-31B Magnesium	1.4	50-60
10	AZ-31B Magnesium	1.4	50-60
11&12	Not Tested.		
13	6061-T6 Aluminum	0.30	8-16
14	6061-T6 Aluminum	0.30	8-16
15	6061-T6 Aluminim	1.4	50-60
16	6061-T6 Aluminum	1.4	50-60
17-24	Not Tested.		
25	Oxygen Free High Cond. Copper	0.20	7-9
26	Oxygen Free High Cond. Copper	0.20	7-9
27	ARMCO Iron		N

TABLE 5-1.
COMPARISON OF SAMPLE MATERIALS
TESTED

Surface Finish			Hardness Rockwell B	Maximum Flatness Deviation		Remarks
	CLA			micro-meter	10 ⁻³ Inches	
Surface	micro-meter	micro-inch				
o Test Interface	0.38	16-18	B-80	-1.3	-0.05	Ground Finish
	0.25	6-14	B-80	----	-----	Ground Finish
	1.0	21-60	B-80	-1.3	-0.05	Ground Finish
	0.63	13-37	B-81	+2.5	+ 0.1	Ground Finish
	0.38	12-17	E-63	-1.3	-0.05	Lathe Cut Finish
	0.48	18-20	E-61	-7.6	-0.3	Lathe Cut Finish
	1.4	50-60	E-62	-5.1	-0.2	Lathe Cut Finish
	1.6	58-68	E-62	-3.8	-0.15	Lathe Cut Finish
	0.29	11-12	F-88	----	-----	Lathe cut finish Center, 2 mm dia, depressed
	0.51	20-20	F-87	-1.3	-0.05	Lathe Cut Finish
	0.91	33-38	F-93	+6.4	+0.25	Lathe Cut Finish
	1.4	50-58	F-93	+2.5	+0.1	Lathe Cut Finish
	0.30	12-12	B-48	+6.4	+0.25	Lathe Cut Finish
	0.42	16-17	B-48	+1.3	+0.05	Lathe Cut Finish

Surfaces for the test interfaces were finished in approximately 0.25, 1.3, and 2.5 x 10⁻⁶ meter (rms) finish (10, 50 and 100 micro-inch-rms). The corresponding Talysurf CLA (center line average) readings are also shown in Table 5-1. Appendix B presents a brief discussion of the several methods of surface finish definition.

The thermocouple holes represented a critical drilling job because of the close dimensional tolerances placed on the axial location of the holes. In fact, a larger drill, as discussed earlier, had to be used in order to reduce runout problems and their attendant inaccuracy.

The test surface finishes were obtained by use of grinding and lathe turning and are listed in Table 5-1. Considerable difficulty was encountered in some cases and rework was required to achieve the desired finishes. After machining each sample was cleaned and handled carefully, using a plastic container for each sample half. A traveling log sheet accompanied each sample half and all subsequent operations and measurements were recorded on it.

In the case of the copper and Armco Iron, the composition and constituents were obtained and are shown separately in Table 5-2. During the thermocouple installation

TABLE 5-2.
COMPOSITION AND CONSTITUENTS OF COPPER AND ARMCO IRON
MATERIAL DATA
AS SUPPLIED BY VENDORS

OHFC Copper

99.96% Copper

Yield Strength 31,830 psi

Tensile Strength 35,480 psi

ARMCO Iron

C 0.019

Mn 0.034

P 0.003

S 0.018

Si 0.004

Cu 0.085

work, the samples were handled carefully so as not to mar the test surfaces. The test surfaces were cleaned with alcohol or similar solvents prior to installation in the test apparatus.

The surface finish (Talysurf) and flatness measurements did not result in any damage to the test interfaces, since these measurements were not performed until after the tests had been completed (except samples No. 15, 16). The fact that these measurements were made after the completion of tests did not affect their adequacy. Deformation of asperities was observable on a very localized basis only.

5.7 SURFACE FINISH MEASUREMENTS

One significant area of interest, which strongly affects the thermal contact resistance is the surface finish of the interface. Surface finish, by definition, can include surface roughness as well as waviness, which are described as microscopic and macroscopic effects (Ref. 3) by primary and secondary waviness (Ref. 5) and as surface roughness and waviness in ASA Standard B46.1-1962, Surface Texture (Ref. 6).

The definition of the last terms as shown in ASA standards is given in Appendix B.

In addition to the small asperities which constitute the roughness, a machined surface can have larger peaks and valleys which constitute the waviness. The direction parallel to the ridges and valleys of the waviness is called the lay direction.

A Taylor-Hobson "Talysurf" stylus-type profilometer was used to obtain single-line profiles of the various surface finishes prepared for this program. Due to difficulties of operating an in-house "Talysurf" instrument, all but one pair of samples (No. 15 and 16) were inspected after thermal contact conductance tests were completed. Any deformation of asperities, which may have taken place during tests would, therefore, be observable. However, it is not very likely that any such effects could be observed because the "Talysurf" trace is merely the record of a stylus motion following the contours of the surface in a straight line. Therefore, any asperity, deformed or otherwise, on either side of this straight line would not be recorded. Although there is no

certainty that a trace parallel to or in continuation to an existing trace will resemble the existing trace, there will be a similarity of characteristics provided the character of the surface is taken into consideration. For example, in the case of a machined surface, traces should be taken in the direction of tool motion as well as in the perpendicular direction. Particular attention needs to be paid in lathe turned finishes at the profile through the center of the surface because of the non-flatness of the surface at that point. Figures 5-11 and 5-12 show two typical "Talysurf" traces.

In order to understand the traces produced by the "Talysurf" instrument, one must recognize the difference in vertical and horizontal scales. An equal magnification in the horizontal stylus travel direction would result in very long traces. For this reason the horizontal scale is fixed and only the vertical magnification has controllable variations as required. The variations used in this study were:

<u>Magnification Number</u>	<u>Magnification</u>	<u>Each Small Vertical Division Equals</u>
3	5000	50×10^{-6} cm (20 μ in.)
4	10000	25×10^{-6} cm (10 μ in.)
5	20000	13×10^{-6} cm (5 μ in.)

Each large horizontal division on the trace equals 0.254 mm (0.01 in.) of stylus travel. These values are shown on the trace strips.

The traces as shown do not represent a true pictorial representation of the surface because of the scale differences. These asperities appear to be much more severe than they are in reality. Nevertheless, the traces do provide a significant amount of useful information and provide an excellent means for comparison of surface finishes.

As a result of the length of the stylus travel (1.27 cm max) which is adjustable, and using the optical flat attachment, flatness deviations can also be observed. This is because the stylus' motion relative to an optical flat is recorded. Figure 5-11 shows a trace about the center of a machined surface for a copper sample, indicating waviness.

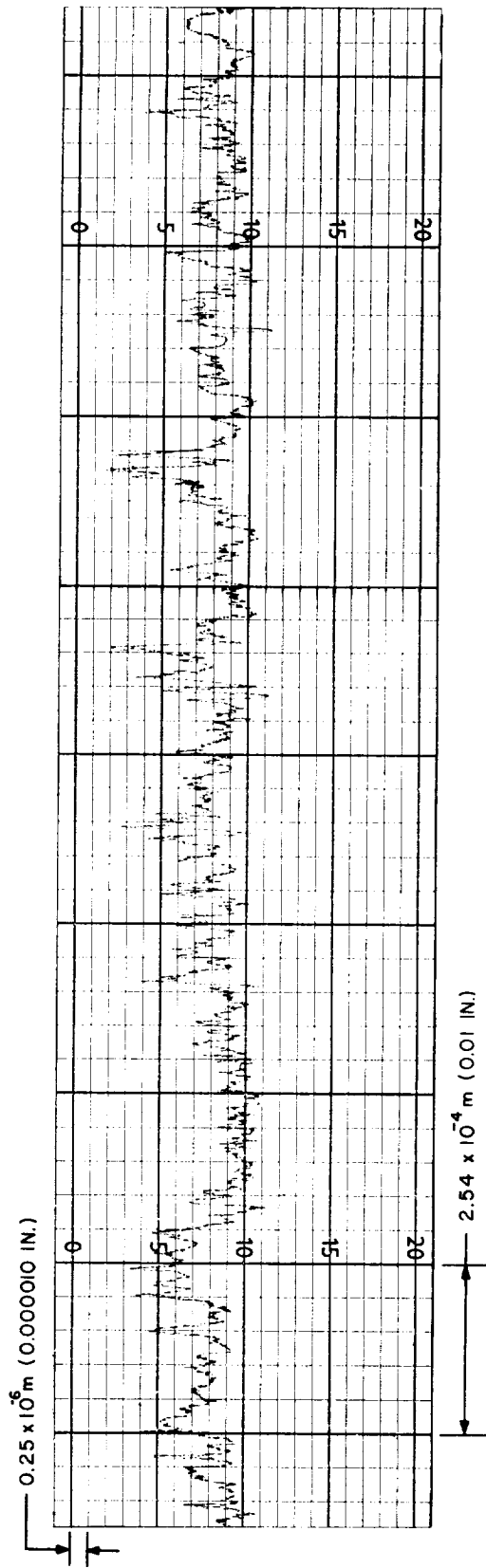


Figure 5-11. Typical Talysurf Trace (Sample 13)

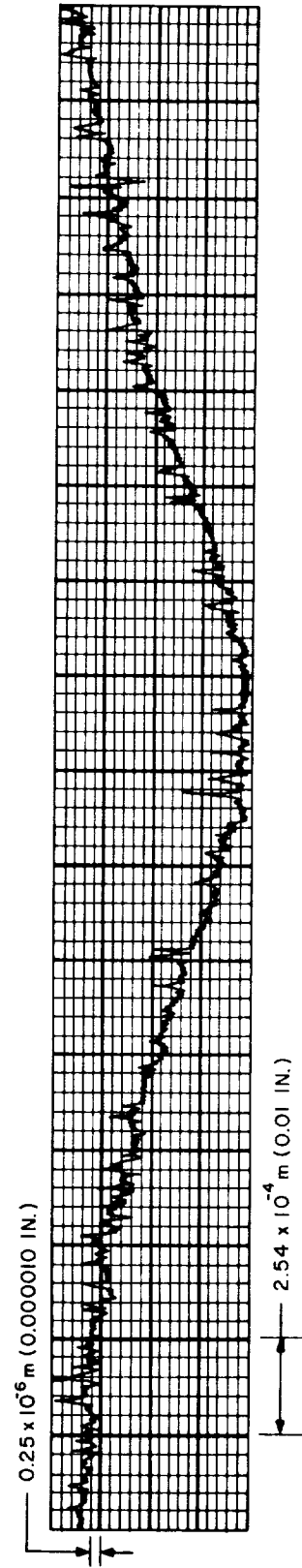


Figure 5-12. Talysurf Trace Showing Waviness (Sample 25)

An additional feature of the "Talysurf" profilometer is its ability to provide a center line average (CLA) roughness reading by means of an electronic integrator circuit for any surface of certain minimum length. The CLA is also known as arithmetic average (AA) and runs somewhat lower than the corresponding root-mean-square (RMS) reading. The latter gives more weight to the larger deviations from the centerline. Appendix B shows the different equations and typical differences for common shapes.

Flatness measurements were made using a surface plate and a dial indicator reading in 2.5×10^{-6} m (0.0001 in.) thus permitting estimation of half divisions (1.3 micrometers). The dial indicator point was set at the sample center and the dial was set at zero. With the dial indicator fixed, the sample was moved so that the point traveled to the sample edge, reading the vertical deviation at the center, 1/4 diameter, and at the edge.

This was done at mutually perpendicular diameters. A secondary check was made initially, by holding the sample fixed and moving the dial indicator support stand. No significant differences were observed between the two methods. Plus readings indicated high spots whereas minus reading indicated low spots. Results are shown in Table 5-1, where the maximum values are presented. It should be noted, that these values are the maximum from a fictitious plane, ie., the datum plane as described in Section 2. Thus, there may occur some matching of interfaces having deviations which could result in a test assembly of better mating than would be expected on the basis of individual reading. For example, samples 3 and 4 could have a cumulative flatness deviation of only $+1.2 \times 10^{-6}$ meters if they fitted into each other.

One interesting observation was made on lathe-turned interfaces. Due to machining procedures, the tool was permitted to dig into the center in samples 13 and 25 resulting in an observable depression (minus reading) at that point. No corrections were made for such events since the area affected represented approximately 1/4 of 1%.

As stated earlier and shown in Figure 5-11, the "Talysurf" trace also is able to show flatness deviations of less than approximately 5 mm diameter.

6. THERMAL TEST RESULTS

The material and the important surface properties of the test samples are shown in Table 5-1. These include roughness, Rockwell hardness, flatness deviation and type of surface preparation.

The estimated accuracy of the test data obtained in this program is better than $\pm 5\%$ at contact pressures about 350×10^3 Newton/m² (≈ 50 psi) and $\pm 10\%$ below that value.

6.1 STAINLESS STEEL 304

Figure 6-1 shows the results of the stainless steel interface tests. Of interest is the large difference in conductance at the maximum contact pressure. The flatness deviation of the 0.30 micrometer (rms) roughness samples (Nos. 1, 2) was 1.3 micrometer, whereas the 1.2 micrometer (rms) roughness sample (Nos. 3, 4) had a flatness deviation of approximately 1.5 micrometer at best and 3.8 at worst, depending on surface matching.

Of interest is the curvature of the fine finish contact conductance curve whose behavior was confirmed by the descending load curve. Some hysteresis could be observed for this specimen for the loading-unloading cycle. In contrast to this the coarse finish sample curve shows no hysteresis and is almost linear.

It is of particular interest to note and compare these two curves in Figure 6-1 with the corresponding results of Clausing (Ref. 3). The resemblance of Clausing's results with stainless-steel 303 for approximately the same degree of flatness deviation with GE's results is remarkable. The importance of the approximate similarity of flatness deviation, as opposed to a marked difference in roughness (Clausing's 3μ in. for both curves versus GE's 12 and 50μ in.) is well demonstrated in this experiment.

6.2 MAGNESIUM

Figure 6-2 shows the results for magnesium AZ31B, a widely used magnesium alloy. These samples, which had lathe turned interfaces, exhibited a rather unusual reversal of expected performance. The coarse finished surfaces exhibited higher thermal contact conductances than did the fine finished interfaces. One possible explanation would be the greater effect of a surface film on a fine finish surface versus that on a coarse finish surface. Oxide films and tarnish were visible on both sets of samples since

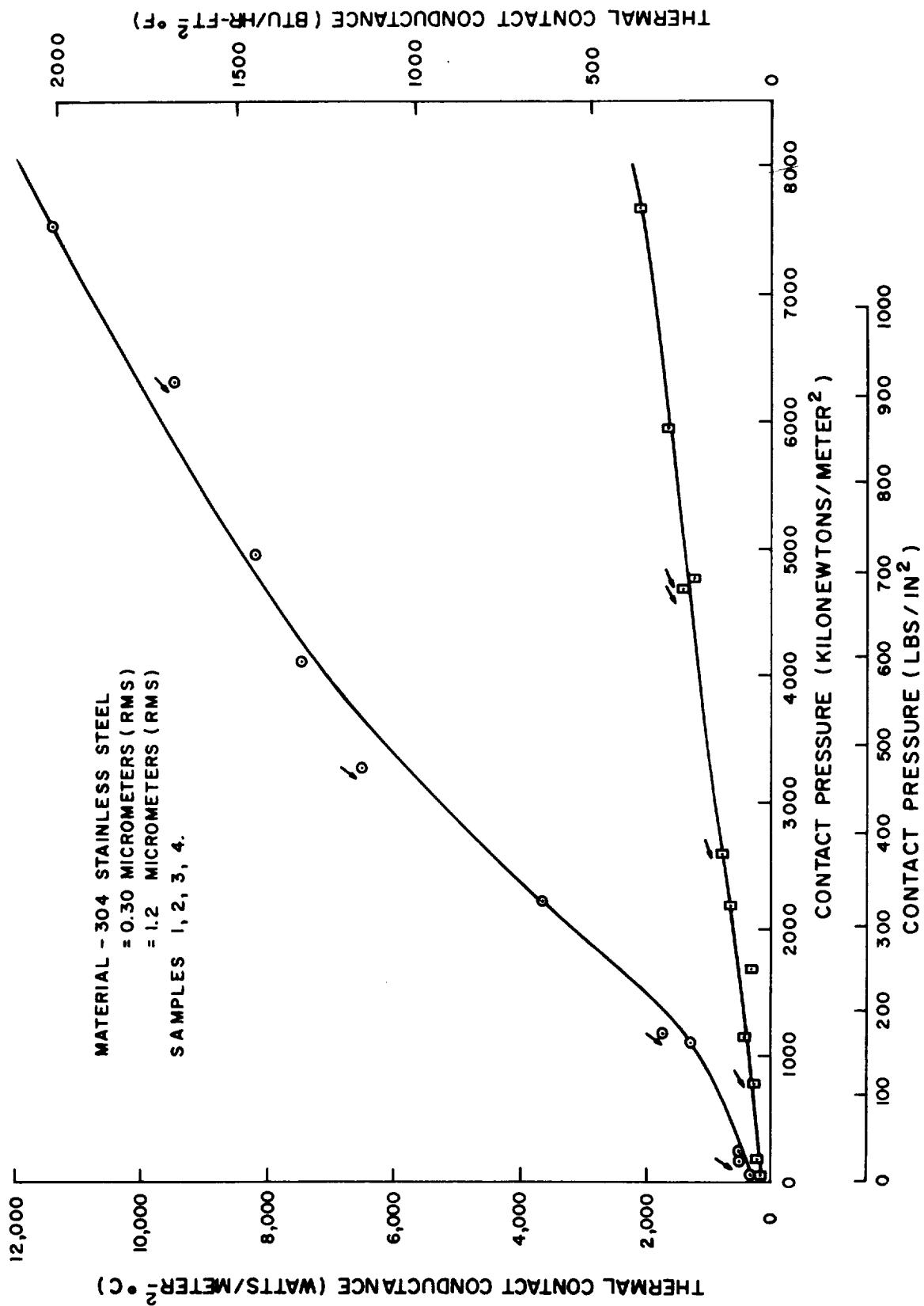


Figure 6-1. Thermal Conductance vs. Contact Pressure - 304SS

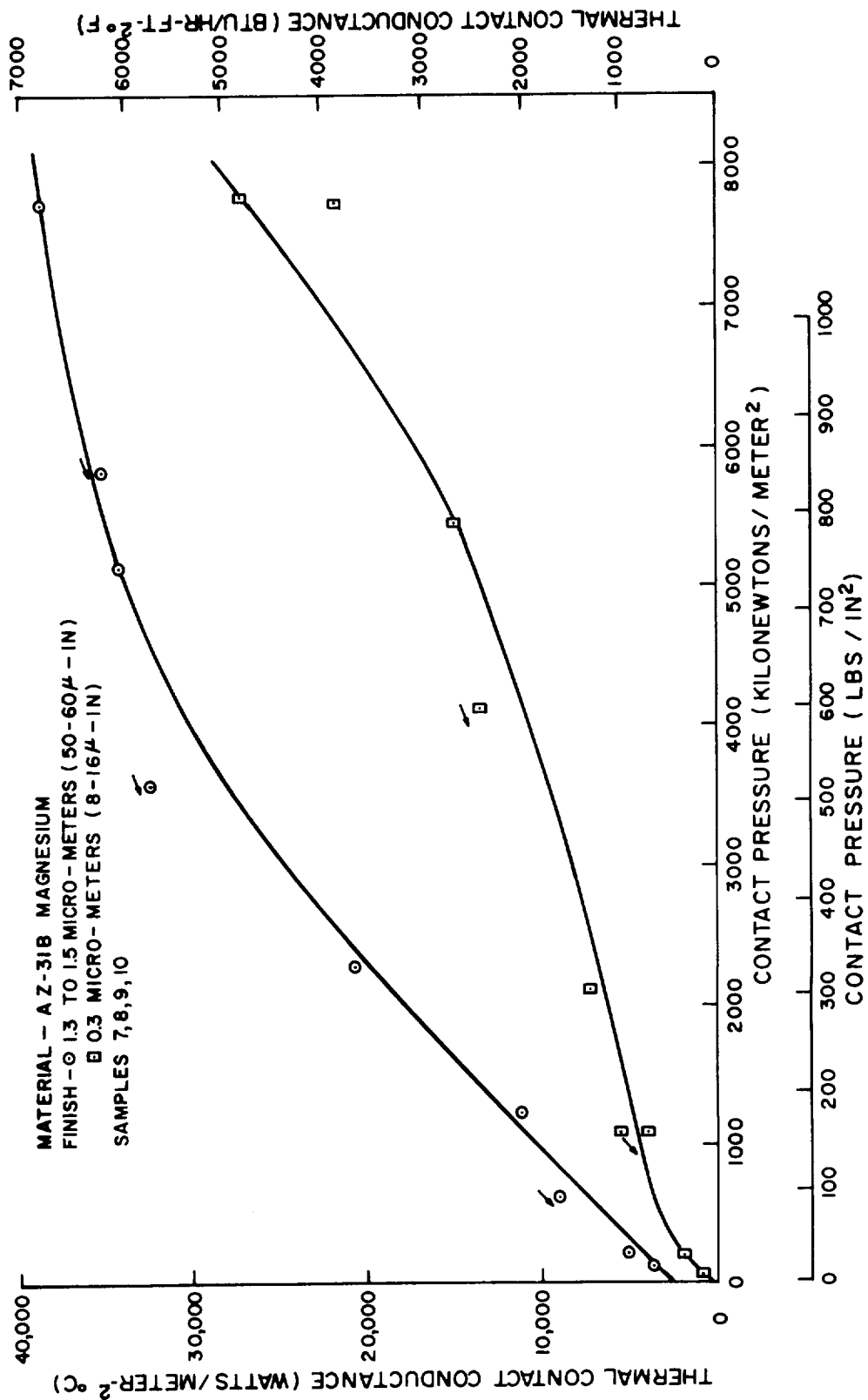


Figure 6-2. Thermal Conductance vs. Contact Pressure - AZ31B Magnesium

2 months had elapsed between machining and test. The reasoning leading to the conjecture, that a film will have a lesser effect on a coarse surface finish, is that the fewer sharper ridges of such a coarse finish will result in higher loads per unit area and cause the film to break. Another, perhaps more plausible reason, is due to the relatively large flatness deviation for both sample pairs, where the resultant sample assembly may have resulted in a greater mismatch leading to the poorer performance.

It is of interest to note that Clausing (Ref. 3) obtained higher thermal conductances for a similar material having lower values of flatness deviation and much lower surface roughness. Clausing also observed film effects and other secondary effects such as creep.

6.3 ALUMINUM

The resultant conductance versus pressure curves are shown in Figure 6-3. It is of interest to note that there was no significant difference in the values of contact conductance for the two surface finishes considered. The results for samples Nos. 13 and 14, the finer (0.3 micrometer rms) finish 6061 T6 aluminum, should have been higher than for the coarse samples Nos. 15 and 16, (1.4 micrometer rms) finish since the former had lower values of flatness deviation, as shown in Table 5-1. At present no explanation can be found for this behavior. The general shape of this curve conforms to that shown by Clausing (Ref. 3) for 2024 Aluminum, with the thermal conductance somewhat lower at maximum pressure. It is planned to conduct further tests on 2024 T4 aluminum in the next contract period to study this problem in more detail.

6.4 COPPER

A thermal conductance test for a joint made of electrical grade OFHC (oxygen free, high conductivity) copper was performed using lathe finished interface surfaces of 0.20 micrometer (rms) roughness. The "Talysurf" trace shown in Figure 5-12 was obtained from this test sample. Of interest is the trace of the dip in the center of the specimen (No. 25), which was due to the machining procedure, i. e. a digging in by the tool.

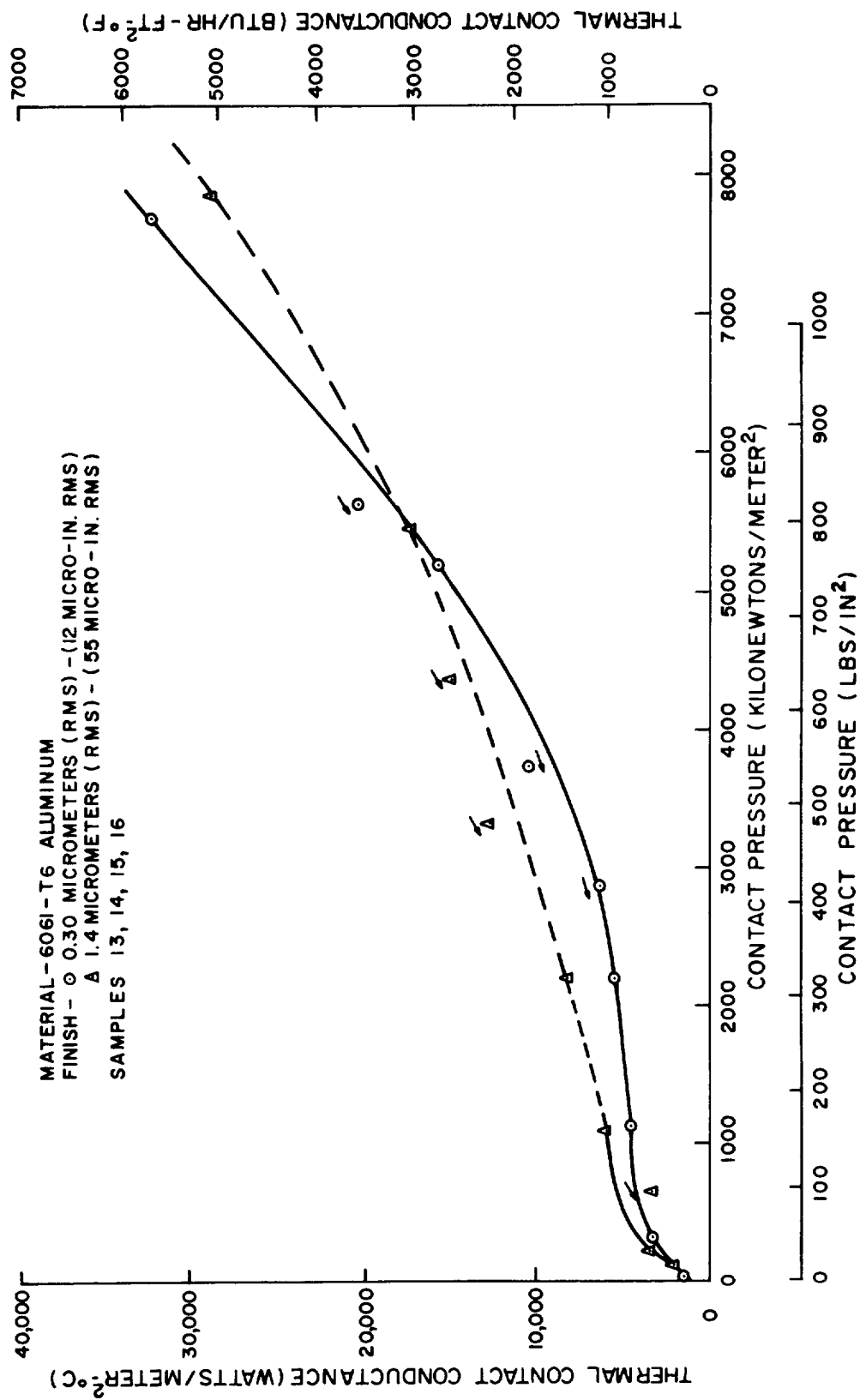


Figure 6-3. Thermal Conductance vs. Contact Pressure - 6061-T6 Aluminum

This test was performed because of lack of reliable data on copper. The only available data Jacobs and Starr (Ref. 18), indicated linear variation of conductance with load at moderate loads, whereas most other materials were observed to change in a non-linear manner in that contact pressure region. The results are not in agreement with Jacobs and Starr.

As can be seen in Figure 6-4 the curve is not linear at low pressures, but does not appear to be linear at higher contact pressures. It is also of interest to note that no hysteresis could be observed for this copper joint specimen.

6.5 GENERAL RESULTS

Table 6-1 shows the measured conductance, pressure, and temperature data in the sequence of the test performance. This data combined with that of Table 5-1 should permit application of possible prediction techniques.

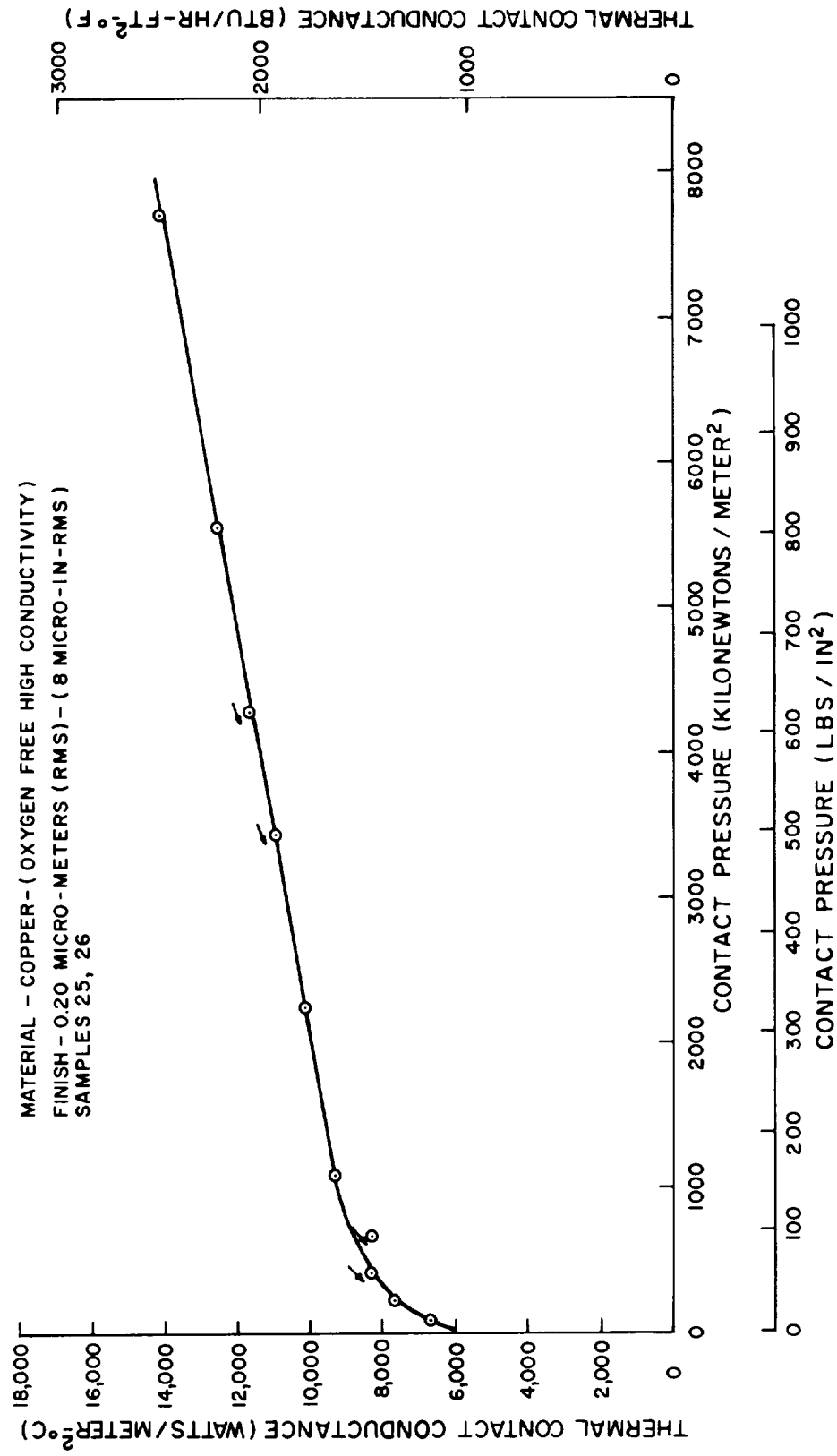


Figure 6-4. Thermal Conductance vs. Contact Pressure - OFHC Copper

TABLE 6-1. COMPARISON OF TEST RUNS

Test Run (No.)	Sample Numbers	Material	Interface Temperatures		Pressure (Kilo-Newton/m ²)	Pressure (PSI)	h _c (Watts/m ² -°C)	h _c (BTU/Hr-Ft ² -°F)
			T ₁ (°C)	T ₂ (°C)				
1	3 & 4	304-SS	19.3	29.3	66	9	210	37
2	3 & 4	304-SS	19.5	27.2	220	32	284	50
3	3 & 4	304-SS	21.2	26.6	1164	169	471	83
4	3 & 4	304-SS	22.0	25.9	2225	323	698	123
5	3 & 4	304-SS	22.9	24.6	5973	867	1704	300
6	3 & 4	304-SS	23.0	24.4	7696	1117	2118	373
7	3 & 4	304-SS	22.8	24.9	4795	696	1369	241
8	3 & 4	304-SS	23.2	25.2	4699	682	1448	255
9	3 & 4	304-SS	22.0	25.4	2611	379	829	146
10	3 & 4	304-SS	20.2	27.5	778	113	312	55
11	3 & 4	304-SS	20.2	29.2	220	32	244	43
12	1 & 2	304-SS	26.4	31.4	55	8	318	56
13	1 & 2	304-SS	22.8	25.9	220	32	523	92
14	1 & 2	304-SS	25.6	27.5	1096	159	1312	231
15	1 & 2	304-SS	25.4	26.1	2192	318	3652	643
16	1 & 2	304-SS	—	—	4960	720	8174	1439
17	1 & 2	304-SS	—	—	7517	1091	11416	2010
18	1 & 2	304-SS	—	—	3259	473	6526	1149
19	1 & 2	304-SS	25.9	27.3	1184	172	1755	309
20	1 & 2	304-SS	29.0	33.3	219	32	545	96
21	1 & 2	304-SS	32.8	33.3	4112	597	7474	1316
22	1 & 2	304-SS	32.8	33.2	6304	915	9497	1672
23	13 & 14	6061-T6 Al.	25.7	32.0	70	10	1556	274
24	13 & 14	6061-T6 Al.	16.2	20.0	313	45	3164	557
25	13 & 14	6061-T6 Al.	24.4	27.1	1123	163	4408	776
26	13 & 14	6061-T6 Al.	24.8	27.1	2191	318	5419	954
27	13 & 14	6061-T6 Al.	24.0	25.2	5208	756	15773	2777
28	13 & 14	6061-T6 Al.	32.0	32.7	7696	1117	32314	5689
29	13 & 14	6061-T6 Al.	31.7	32.9	5649	820	20408	3593
30	13 & 14	6061-T6 Al.	31.4	33.7	3761	546	10235	1802
31	13 & 14	6061-T6 Al.	31.6	35.5	2886	419	6055	1066
32	9 & 10	AZ-31B Mag	28.3	37.5	110	16	3868	681
33	9 & 10	AZ-31B Mag	29.4	32.5	220	32	5061	891
34	9 & 10	AZ-31B Mag	28.6	29.9	1195	173	10979	1933
35	9 & 10	AZ-31B Mag	35.2	36.1	2280	331	20607	3628
36	9 & 10	AZ-31B Mag	38.7	39.3	5133	745	34171	6016
37	9 & 10	AZ-31B Mag	43.0	43.7	7696	1117	38596	6795
38	9 & 10	AZ-31B Mag	43.4	44.1	5801	842	35375	6228
39	9 & 10	AZ-31B Mag	42.8	43.5	3582	520	32535	5728
40	9 & 10	AZ-31B Mag	43.3	45.9	627	91	9014	1587
41	25 & 26	Copper	45.7	52.4	65	9	6708	1181
42	25 & 26	Copper	45.5	51.5	220	32	7446	1311
43	25 & 26	Copper	45.2	50.1	1095	159	9270	1632
44	25 & 26	Copper	45.2	50.7	2280	331	10099	1778
45	25 & 26	Copper	44.1	47.7	5560	807	12507	2202
46	25 & 26	Copper	44.3	47.4	7696	1117	14171	2495
47	25 & 26	Copper	44.5	48.3	4285	622	11700	2060
48	25 & 26	Copper	44.2	48.2	3424	497	10990	1935
49	25 & 26	Copper	44.2	49.6	658	95	8270	1456
50	25 & 26	Copper	44.2	49.6	394	57	8201	1444
51	7 & 8	AZ-31 Mag	30.6	44.3	65	9	1073	189
52	7 & 8	AZ-31 Mag	31.7	39.2	219	31	1988	350
53	7 & 8	AZ-31 Mag	30.1	33.8	1096	159	4066	716
54	7 & 8	AZ-31 Mag	41.3	44.3	2116	307	7304	1286
55	7 & 8	AZ-31 Mag	41.5	42.9	5461	792	15069	2653
56	7 & 8	AZ-31 Mag	41.8	42.7	7785	1130	27451	4833
57	7 & 8	AZ-31 Mag	45.5	47.3	4112	596	13722	2416
58	7 & 8	AZ-31 Mag	41.8	45.8	1095	159	5492	967
59	7 & 8	AZ-31 Mag	41.7	42.7	7696	1117	21987	3871
60	—	Armco Iron	—	—	—	—	—	—
61	15 & 16	Al. 6061-T6	32.3	45.1	131	19	1999	352
62	15 & 16	Al. 6061-T6	32.5	39.9	219	31	3431	605
63	15 & 16	Al. 6061-T6	39.5	45.6	1095	159	5282	930
64	15 & 16	Al. 6061-T6	39.9	43.9	2193	318	8071	1421
65	15 & 16	Al. 6061-T6	47.6	49.8	5465	793	17244	3036
66	15 & 16	Al. 6061-T6	47.7	49.0	7873	1142	28712	5055
67	15 & 16	Al. 6061-T6	47.9	50.4	4375	635	15040	2649
68	15 & 16	Al. 6061-T6	48.2	51.2	3340	484	12575	2215
69	15 & 16	Al. 6061-T6	41.1	49.4	658	95	3680	648

7. GENERAL REMARKS AND CONCLUSIONS

When conductance versus pressure is plotted on log-log paper, a curve as shown in Figure 7-1 results which is somewhat different from earlier observed and expected results. Initially a slope of $1/2$ to $2/3$ was expected for elastic behavior as discussed in another section of this paper. However, plots of data obtained in this study indicate a definite two-regime behavior with a pronounced point of change in slope for most of the test results. The exact reason for this change in slope has not yet been defined, although it is believed that possibly it represents the change from purely elastic to elastic-plastic deformation behavior. It is planned to investigate this phenomenon in greater detail. Since the amount of experimental data suitable for such further investigation is presently limited, the experimental work will continue and should provide a substantial number of suitable data points. This will also be supplemented by data from other investigators. It is anticipated that the above observation may lead to a semi-empirical method of thermal contact conductance prediction. The recently proposed method of Clausing (Ref. 3) will also be tried with the MSD current data and may well be adopted if it is found to provide satisfactory results, or modified if found

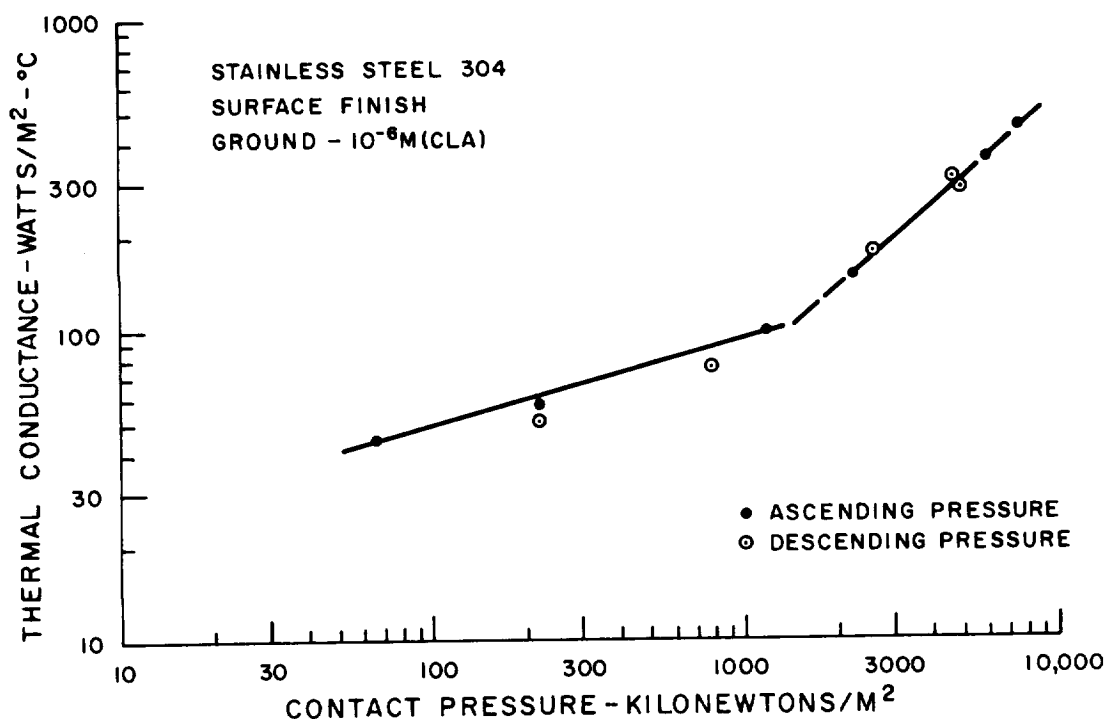


Figure 7-1. Thermal Conductances Log-Log Plot, Stainless-Steel 304

desirable. The difficulty of implementing the present Fenech and Rohsenow (Ref. 2) method makes it practical to wait for further progress on their study to make it easier to use. Both of the above methods appear to have merit.

The following, more or less reasonable, conclusions are made on the basis of the reported study.

1. Existing methods of thermal contact conductance prediction are not readily applicable to surfaces as currently defined.
2. Proposed models of engineering surfaces based on the elastic deformation relations of Hertz appear to provide an approach to an understanding of the heat-transfer prediction for mating surfaces in vacuum.
3. There appears to exist a two-regime behavior, when thermal conductance is plotted against load on log-log paper. This could represent a change from purely elastic to elastic-plastic behavior and deserves further study.
4. The work carried out in this study and by other investigators has indicated a need for a "round robin" test specimen to aid in obtaining a common basis of test procedures and result definition.
5. More experimental data of suitable accuracy is needed to arrive at:
 - a. Evaluation of prediction techniques
 - b. Statistical correlations.
6. Flatness deviation (macroscopic constriction) effects were noted to be of significance in controlling the thermal conductance of metallic contacts in vacuum. This is particularly true as the length-to-diameter ratio of the test specimen becomes small.
7. Present methods of surface definition and surface measurement are not suitable for thermal contact conductance prediction. More precise definitions and a method of standardization of these definitions are required.

8. REFERENCES

1. "Electrical Contacts Handbook," R. Holm, 3rd Ed., Springer Verlag, Berlin (1958)
2. "Prediction of Thermal Conductance of Metallic Surfaces in Contact," H. Fenech and W.M. Rohsenow, Journal of Heat Transfer, Vol. 85, p. 15-24 (Feb. 1963)
3. "Thermal Contact Resistance in a Vacuum Environment," A.M. Clausing and B.T. Chao, University of Illinois, Report ME-TN-242-1, (Aug. 1963)
4. "Interface Thermal Contact Resistance Problem in Space Vehicles," E. Fried and F.A. Costello, ARS Journal, Vol. 32, No. 2, p. 237 (1962)
5. "Thermal Conductance of Metallic Surfaces in Contact," H. Fenech and W.M. Rohsenow, U.S. Atomic Energy Commission Report NYO-2136, (May 1959)
6. "American Standards Association, Surface Roughness, Waviness, and Lay," ASA Standards B46.1 (1962)
7. "Thermal Contacts - Simplified Theory and Rules for Calculations," R. Holm Memo (Oct. 1963)
8. "Thermal Resistance of Metal-to-Metal Contacts: An Annotated Bibliography," Compiled by R.C. Gex, ASTIA Document 263181, (July, 1961)
9. "Thermal Conductance of Metal Surfaces in Contact," T.N. Cetinkale and M. Fishenden, General Discussion of Heat Transfer, Proceedings Institute of Mechanical Engineers, ASME, p. 271 (1951)
10. "Thermal Resistance Measurements of Joints Formed Between Stationary Metal Surfaces," N.D. Weills and E.A. Ryder, Transactions ASME, Vol. 71, No. 3 (1949)
11. "Thermal Contact Resistance of Laminated and Machines Joints," A.W. Brunot and F.F. Buckland (Mrs.), Transactions ASME, Vol. 71, No. 3 (1949)
12. "Thermal Resistance of Metal Contacts," W.B. Kouwenhoven and J.H. Potter, Welding Journal, Vol. 27, p. s155-s205 (1948)
13. "Thermal Conductance of Contacts in Aircraft Joints," M.E. Barzelay, Kin Nee Tong, and G.F. Holloway, NACA TN 3167 (1954)
14. "Effects of Pressure on Thermal Conductance of Contact Joints," M.E. Barzelay, Kin Nee Tong, and G.F. Holloway, NACA TN 3295 (1955)
15. "Range of Interface Thermal Conductance for Aircraft Joints," M.E. Barzelay, (Syracuse University) NASA TN D-426, (May, 1960)

16. "Interface Thermal Conductance of 27 Riveted Aircraft Joints," M.E. Barzelay, and G. F. Holloway NACA TN 3991, (1957)
17. "Thermal Conductance of Machines Metal Contacts," L.C. Laming ASME-International Heat Transfer Conference, Boulder, Colorado, Paper No. 8 (1961)
18. "Thermal Conductance of Metallic Contacts," R.B. Jacobs and C. Starr, Rev. Scientific Instrument, Vol. 10 (1939), p. 40
19. "The Thermal Conductance of Contacts Between Aluminum and Other Metals," F. Boeschoten and E. F. M. Van Der Held, Physica 23 (1957)
20. "Thermal Conductance of Fuel Element Materials," R.G. Wheeler, Hanford Atomic Products Operation (AEC) Reports HW 60343 (1959) and HW 53598 (1957)
21. "Measurement of the Thermal Contact Resistance Between Flat Surfaces of Uranium and Aluminum," A. Ascoli and E. Germagnoli, Energia Nucleare (Italian) Vol. 3, No. 1, p. 23-31, February 1961. Transl. RSIC-99
22. "Consideration of the Thermal Contact Resistance Between Facing Flat Metal Surfaces," A. Ascoli and E. Germagnoli, Energia Nucleare (Italian) Vol. 3 No. 2, p. 113-118, April 1956
23. "Thermal Contact Resistances," C. Bory and H. Cordier, Institut Francois des Combustibles et de L'Energie, (1961)
24. "Thermal Joint Conductance in a Vacuum," E. Fried, ASME Paper 63-AHGT-18 (April 1963)
25. "The Heat Transfer Properties of Structural Elements for Space Instruments," R.M. Jansson, MIT Instrumentation Lab Report E-1173 (June 1962)
26. "Elastic Deformation and the Laws of Friction," J. F. Archard Royal Soc. of London Proceedings A Vol. 243 - p. 190 (1957)
27. "Controlling Factors of Thermal Conductance Across Bolted Joints in a Vacuum," W. Aron and G. Colombo, ASME Paper 63-W-196, (Nov. 1963)
28. "A Brief Bibliography Concerning Thermal Contact Conductance," H. Atkins, Ed., R-RP-INT-64-8 NASA-Internal Note
29. "The True Contact Area Between Solids," J. Dyson and W. Hirst, Proc. Phys. Soc. Sec "B", Vol 67, p. 309 (1954)
30. "Heat Transfer at the Interface of Dissimilar Metals," G. F. C. Rogers, Int. Jour. Heat and Mass Transfer Vol. 2, p. 150, 1961
31. "Der Wärmeübergang Zwischen bearbeiteten Oberflächen," W. Held, Allgemeine Wärmetechnik, Vol. 8, No. 1, p. 1 (1957)

32. Letter to Editor, A. Williams, Int'l. Jour. Heat and Mass Transfer, Vol. 3, p. 159, (1962)
33. "Characterization of Surface Roughness," N.O. Myers, Wear Vol. 5, p. 182-9, (1962)
34. "Measuring Surface Finish - State-of-the-Art Report," J. B. Bryan, G.I. Boyadjieff, and E.R. McClure, Mechanical Eng'g, p. 42, Dec. 1963.

9. NOMENCLATURE

A = Area
h = Heat transfer Coefficient
Z = Heat Flow
q = Heat Flow per unit area
a = Accommodation coefficient
p = Pressure
R₀ = Universal Gas Constant
M = Molecular weight of gas
k = Thermal Conductivity
m = Ratio of actual to nominal contact area
T = Temperature
R = Resistance - Thermal
x = Axial dimension
P = Load
B = Constant in Equation (11)
Y₀ = Yield Strength
N = Number of contact spots

Greek Letters

α = absorptivity
 ϵ = emissivity
 σ = Stefan-Boltzman constant
 δ = gap thickness
 γ = ratio of specific heats
 β = exponents

Subscripts

f = fluid
s = solid
r = radiation
1, 2 = sample surfaces of interest
c = contact

APPENDICES

APPENDIX A

THE CONTACT MECHANISM

When two flat surfaces make contact, the real area of contact is formed by the elastic and plastic deformation of the contacting surface protuberances under the applied load. On the basis of the Hertz theory of the deformation of a spherical protuberance pressed against a flat plate, one can state that for the purely elastic case the real area

$$A = BP^{2/3}, \quad (A-1)$$

where B is a constant and P is the applied load. For the case of plastic deformation, the area will be proportional to the load.

Archard (Ref. 26) reports on theoretical studies carried out in the past.

If one assumes that deformation is entirely elastic, a more general form of equation A-1 will be required for surfaces touching in many places. Archard suggests

$$A = BP^{\beta} \quad (A-2)$$

where β depends on the curvature, elastic properties and other surface parameters and has a value between 2/3 and 1. Depending on the theoretical model chosen, Archard shows values of β increasing to unity as the number of spherical segment making up the surface increases. Thus, for the Hertz model of a single spherical contact, the total number of individual contacts N is constant, whereas for the multiple microscopic spherical segments superposed on the larger, macroscopic segments, N as well as A is proportional to P, with β varying between 2/3 and 1. Archard states that as the complexity of the model increases, the number of individual areas approaches proportionality with load, whereas their size becomes less dependent upon it. Dyson and Hirst (Ref. 29), reporting measurements on lapped surfaces, show that the contact area size was almost independent of applied load.

There exist a number of excellent treatises on the relation between applied load and surface contact area. These will be studied in detail during the continuation of the present program.

APPENDIX B

SURFACE DEFINITIONS AND STANDARDS

Existing techniques for surface examination, definition and specification are inadequate for the requirements of this or similar studies.

The most commonly used standard is ASA-B46-1-1962 - Surface Texture. The following excerpts are shown to delineate the scope of this standard and some definitions.

- "1.1 This standard is concerned with the geometric irregularities of surfaces of solid materials, physical specimens for gaging roughness, and the characteristics of instrumentation for measuring roughness. It establishes definite classifications for roughness, waviness, lay, and a set of symbols for drawings, specifications, and reports. In order to assure a uniform basis for measurement, it also provides specifications for Precision Reference Specimens, Roughness Comparison Specimens, and establishes requirements for Tracer Type instruments.

"This standard is not concerned with luster, appearance, color, corrosion resistance, wear resistance, hardness, micro-structure, and many other characteristics which may be governing considerations in specific applications.
- "1.2 This standard does not define the degrees of surface roughness and waviness or type of lay suitable for specific purposes, nor does it specify the means by which any degree of such irregularities may be obtained or produced. However, criteria for selection of surface qualities and information on instrument techniques and methods of producing, controlling and inspecting surfaces are included in Appendixes A, B, C and D, which are not an integral part of this standard.
- "1.3 Surfaces, in general, are very complex in character. This standard deals only with the height, width, and direction of surface irregularities, since these are of practical importance in specific applications."
- "2.6 Roughness. Roughness consists of the finer irregularities in the surface texture usually including those irregularities which result from the inherent action of the production process. These are considered to include traverse, feed marks and other irregularities within the limits of the roughness-width cutoff.
- "2.6.1 Roughness Height. For the purpose of this standard, roughness height is rated as the arithmetical average deviation expressed in microinches measured normal to the center line.

- "2.6.2 Roughness Width. Roughness width is the distance parallel to the nominal surface between successive peaks or ridges which constitute the predominant pattern of the roughness. Roughness width is rated in inches.
- "2.6.3 Roughness-Width Cutoff. The greatest spacing of repetitive surface irregularities to be included in the measurement of average roughness height. Roughness-width cutoff is rated in inches. Standard values are given in *Table 2. Roughness-width cutoff must always be greater than the roughness width in order to obtain the total roughness height rating.
- "2.7 Waviness. Waviness is the usually widely-spaced component of surface texture and is generally of wider spacing than the roughness-width cutoff. Waviness may result from such factors as machine or work deflections, vibration, chatter, heat treatment or warping strains. Roughness may be considered as superposed on a "wavy" surface.
- "2.7.1 Waviness Height. Waviness height is rated in inches as the peak to valley distance.
- "2.7.2 Waviness Width. Waviness width is rated in inches as the spacing of successive wave peaks or successive wave valleys. When specified, the values shall be the maximum permissible.
- "2.8 Lay. The direction of the predominant surface pattern, ordinarily determined by the production method used.
- "2.9 Flaws. Flaws are irregularities which occur at one place or at relatively infrequent or widely varying intervals in a surface. Flaws include such defects as cracks, blow holes, checks, ridges, scratches, etc. Unless otherwise specified, the effect of flaws shall not be included in the roughness height measurements."

The centerline average (CLA) value given for the surfaces on the basis of Talysurf ratings is defined by:

$$CLA = \frac{1}{\ell} \int_{x=0}^{x=\ell} |Y| dx .$$

This is in contrast to the root-mean-square (rms) value defined by:

$$RMS = \frac{1}{\ell} \left[\int_{x=0}^{x=\ell} Y^2 dx \right]^{1/2} .$$

*The Table referred to lists standard roughness-width cutoff values of 0.003 in., 0.010 in., 0.030 in., 0.100 in., 0.300 in. and 1.000 in. When no value is specified the value 0.030 is assumed.